Accumulation and Mobility of Radionuclides in the Sellafield Near-Shore

A thesis submitted to the University of Manchester for the degree of Master of Science by Research in the Faculty of Engineering and Physical Sciences

2013

Daisy Ray

School of Chemistry

Contents

Contents 2

List of Figures 5

Abstract 7

Declaration 8

Copyright 8

Chapter 1 Introduction 10

1.1. Overview 11

1.2. Thesis Structure 11

1.3. Nuclear Power 12

1.3.1 Early Development and Contemporary Demand 12

1.3.2. The UK Nuclear Legacy 13

1.4. The Nuclear Fuel Cycle 14

1.4.1. Mining and Milling of Uranium Ore 15

1.4.2. Purification and Fuel Fabrication 15

1.4.3. Reactor Operation 16

1.4.4. Spent Fuel Reprocessing 17

1.5. Sellafield 19

1.5.1. Operational History of Sellafield 19

1.6. Radionuclides in the Environment 20

1.6.1. Authorised Sellafield Discharges 21

1.7. The Chemistry of Select Actinides and Fission Products in Sellafield Effluents 23

1.7.1. Plutonium 23

1.7.2. Americium 26

1.7.3. Caesium 27

1.8. Biogeochemistry of the Natural Environment 27

1.8.1. Sorption 28

1.8.2. Incorporation/Precipitation 29

1.8.3. Redox Reactions 29

1.8.4. Bioturbation 30

1.8.5. Microbial Activity 31

1.9. Mechanism of Radionuclide Transportation 33

1.10. Project Aims 35

Chapter 2 Materials and Methods 37

2.1. Sample Collection 38

2.2. Major and Minor elemental analysis 39

2.3. Americium and Caesium Detection 40

2.3.1. Gamma Spectroscopy Theory 41

2.3.2. Gamma Spectroscopy Procedure and Analysis 42

2.4. Plutonium Detection 43

2.4.1. Alpha Spectroscopy Theory 43

2.4.2. Ion Exchange Resin 45

2.4.3. Alpha Spectroscopy Procedure and Analysis 46

2.4.3.1. Chemical Separation of Plutonium 46

2.4.3.2. Electrodeposition of Pu 48

Chapter 3 Results and Discussion 50

3.1. Biogeochemistry of the Ravenglass Sediment Core 51

3.2. Contemporary Radionuclide Distribution in the Ravenglass Sediment Cores 54

3.2.1. Caesium 55

3.2.2. Americium 58

3.2.3. Plutonium 61

3.2.3.1. Plutonium-239/240 61

3.2.3.2. Plutonium-238 64

3. 3. Comparison of Contemporary Radionuclide Profiles with Previous Data 66

3.3.1. Caesium 66

3.3.2 Americium 68

3.3.4. Plutonium-239/240 70

3.3.3. Plutonium-238 71

Chapter 4 Conclusions and Recommendations for Future Work 75

4.1. Conclusions 76

4.2. Limitations and Recommendations for Further Work 77

References 80

Appendices 93

List of Figures

Figure 1. The nuclear fuel cycle 14

Figure 2. Discharge of ^{137}Cs (TBq) and ^{241}Am (kg) in liquid effluent from Sellafield between 1955-1990 (taken from Kershaw et al., 1992). 22

Figure 3. Discharge of ^{238,239,240}Pu (TBq) in liquid effluent from Sellafield between 1955-1990 (taken from Kershaw et al., 1992). 22

Figure 4. Key geochemical processes that influence the speciation of radionuclides in the environment (Brookshaw et al., 2012). 28

Figure 5. The microbially-mediated redox cascade, showing the net free energy gain associated with each electron acceptor per half reaction, in kcal per mol of carbon oxidised at pH 7 (taken from Stumm and Morgan, 1996). 32

Figure 6. Distribution of sediment types in the Irish Sea, in the vicinity of the Sellafield site by grain size (Pantin, 1991). 34

Figure 7. Sampling site at the Ravenglass saltmarsh. 38

Figure 8. A typical environmental Pu α-spectrum. 44

Figure 9. Concentration (wt %) of (A) Al; (B) Si; (C) Mg; (D) K; (E) Ti; (F) Mo ($x10^3$); (G) Mn/Al ($x\ 10^2$); (H) Fe/Al (x 10), and (I) extractable Fe (mg g^{-1} of sediment) in Ravenglass saltmarsh sediments from 0-25.5 cm. 52

Figure 10. (A) Annual authorised discharge of ^{137}Cs into the Irish Sea from the Sellafield site between 1952-1992 (data from Gray et al., 1995); (B) ^{137}Cs activity profile in the Ravenglass saltmarsh from 0-25.5 cm depth (Appendix 2). Counting errors are ±1σ and if not visible are hidden by the symbol. 57

Figure 11. (A) Annual authorised discharge of ^{241}Am and ^{241}Pu activity into the Irish Sea from the Sellafield site between 1952-1992 (data from Gray et al., 1995); (B)

Measured activity profile for ^{241}Am in the Ravenglass saltmarsh core (Appendix 2). Counting errors (±1σ) are shown but may be shadowed by markers. 59

Figure 12. (A) Annual authorised discharge of ^{239,240}Pu into the Irish Sea from the Sellafield site between 1952-1992) (data from Gray et al., 1995); (B) Measured activity profile for ^{239,240}Pu in the Ravenglass saltmarsh core (Appendix 2). Counting errors (±1σ) are shown but may be shadowed by markers. 63

Figure 13. (A) Annual estimate of ^{238}Pu activity into the Irish Sea from the Sellafield site between 1952-1992 (data from Kershaw et al., 1990); (B) Measured activity profile for ^{238}Pu in the Ravenglass saltmarsh core (Appendix 2). Counting errors (±1σ) are shown but may be shadowed by markers. 65

Figure 14. The temporal variation of ^{137}Cs core profiles for Ravenglass estuarine sediments, spanning three decades. Data is taken from this study, Morris (1996), and Marsden et al., (2004). 67

Figure 15. The temporal variation of ^{241}Am core profiles for the Ravenglass sediments, spanning three decades. Data is taken from this study, Morris (1996), and Marsden et al., (2006) 69

Figure 16. The temporal variation of ^{239,240}Pu core profiles for Ravenglass estuarine sediments, spanning three decades. Data is taken from this study, Morris (1996), and Marsden at al., (2006). 71

Figure 17. The temporal variation of ^{238}Pu core profiles for Ravenglass sediments, spanning three decades. Data from this study, Morris (1996), and Marsden et al., (2006). 72

Abstract

The authorised pipeline discharge of Low Level Waste (LLW) from Sellafield into the Irish Sea has been taking place since operations commenced in 1952 until termination of the effluent discharge took place in 1992. As a consequence of this activity, radionuclides such as caesium (Cs), americium (Am), plutonium (Pu) and neptunium (Np) that were present in liquid effluents, have been transported in marine waters and become associated with sediments in the Irish Sea. Tidal currents coupled with biological processes have then resulted in the redistribution and deposition of these radionuclides in intertidal areas on the West Cumbrian coastline. The Ravenglass saltmarsh, in particular, has received significant radionuclide inputs during tidal processes. This, coupled with the fine-grained sedimentology of the saltmarsh has resulted in the accumulation of actinides and fission products in estuarine sediments. In past work, the mobility and accumulation of these contaminants has been interpreted by natural geochemical processes and correlated with maximum discharge histories from the 1970s.

In this project, a sediment core was taken from the Ravenglass saltmarsh, located by the mouth of River Esk, 5 km from the Sellafield site. Gamma spectroscopy was used to measure the activities of ^{137}Cs and ^{241}Am in the core and isotopes of Pu were determined by α-spectroscopy after chemical separation and electrodeposition. The depth profiles obtained for ^{137}Cs, ^{241}Am, and Pu isotopes all showed elevated activities in the middle of the core (11-13 cm). This reflects the heightened discharges that took place from Sellafield in the 1970's and the burial of the contaminants with time. The similarity in shape of the depth profiles with those measured in previous decades may be indicative of the lack of post-depositional remobilisation taking place in estuarine sediments.

Declaration

No portion of the work referred to in this thesis has been submitted in support of any other application for another degree or qualification of this or any other institute of learning.

Copyright

Acknowledgements

I would like to thank my supervisor Gareth Law for his motivational words throughout the year.

My co-supervisors; Francis Livens and Nick Bryan, thank you for your guidance.

Katie Law, thank you for getting me through α-spectroscopy.

Chapter 1
Introduction

1.1. Overview

The UK's nuclear industry is currently attempting to decommission and dispose of over half a century's nuclear infrastructure and waste. The waste which has resulted from nuclear facilities (e.g. Sellafield) has found its way into local environments *via* authorised disposal into marine waters. Further, it is important to understand radionuclide behaviour as it has a significant radiological impact on the local ecosystem. Undoubtedly, nuclear wastes which have been discharged and have now been deposited in coastline areas, contain radioactive materials. These include Cs, Am, and Pu which are highly radioactive, and due to their long half-life remain in the environment. Consequently over time, they have become bound to intertidal sediments in Cumbrian estuaries and as the saltmarsh is a public location it is important to routinely monitor activities at this site.

1.2. Thesis Structure

This chapter begins with a background on Nuclear Power and the UK's Nuclear Legacy (§ 1.3). Following this, there is a discussion on the Nuclear Fuel Cycle (§ 1.4). Thereafter, Sellafield is introduced with a short account on its operational history (§ 1.5). Then the sources of radionuclides to the environment are discussed, in particular the authorised discharges from Sellafield (§ 1.6). A brief section follows on the chemistry of actinides and fission products that are present in nuclear wastes and the sample site (§ 1.7). Further, there is discussion on the biogeochemistry of the natural environment including, radionuclide sorption, incorporation, redox reactions and microbial activity (§ 1.8). Following this there is a brief discussion on the mechanism of radionuclide transport in the Irish Sea. The end of Chapter 1 discusses the project aims and the motivations for this study.

Chapter 2 (Materials and Methods) begins with a short account on sample collection from the Ravenglass saltmarsh (§ 2.1). This is followed by the method used to determine the concentration of total reactive Fe in the Ravenglass sediments and the use of XRF in major and minor elemental analysis (§ 2.2). A short discussion follows on Am and Cs measurement detection *via* γ-spectroscopy (§ 2.3). Thereafter Pu measurement by α-spectroscopy is discussed at the end of Chapter 2 (§ 2.4).

Chapter 3 begins with biogeochemical evidence, illustrating the concentration of major and minor elements in the sediments (§ 3.1). This is followed by the core profiles for ^{137}Cs, ^{241}Am, $^{239,240}Pu$ and ^{238}Pu that are compared with Sellafield's authorised discharge record (§ 3.2). The end of Chapter 3 compares the core profiles to previous literature (§ 3.4). A brief conclusions and recommendations section closes the thesis (Chapter 4).

1.3. Nuclear Power

1.3.1 Early Development and Contemporary Demand

In 1939 Hahn, Strassmann and Meitner discovered that bombarding uranium (U) with neutrons yielded not only transuranic metals but also a number of elements whose relative atomic masses were exactly half that of U (Hahn and Strassmann, 1939). Thereafter Meitner collaborated with a fellow Austrian, Frisch, to rationalise the initial findings (Meitner and Frisch, 1939). Such early experiments represented mans initial understanding of nuclear fission and supported the realisation that more than one neutron could be produced during fission. The subsequent neutron release created a spontaneous chain reaction, capable of releasing vast amounts of energy;

this is now the central process used to harness energy in a nuclear reactor (Choppin et al., 2002).

From these early beginnings, nuclear power is now a recognised global source of energy, supplying ~ 17 % of the world's power (Joyce and Port, 1999). Indeed, there are currently 450 reactors operational worldwide, with the majority sited in UK, France, Russia, Canada, and the United States (Joyce and Port, 1999). France in particular has recognised the potential of nuclear power as an energy form; here, 75 % of the country's electricity is supplied by nuclear reactors (Wilson, 1996). Developing countries have also seen a large and ever increasing demand for electricity and with the current environmental stance to support low carbon energies, this has lead to a so-called global 'nuclear renaissance' (Choppin et al., 2002).

1.3.2. The UK Nuclear Legacy

Due to over half a century's nuclear power and weapons production in the UK, it is no doubt that an extensive, highly challenging nuclear legacy is present. The Calder Hall reactor represented the start of UK's nuclear timeline, being the first nation to implement nuclear power generation. Currently there are 10 operating nuclear power reactors in the UK, generating ~ one fifth of the country's electricity (NDA, 2011). The UK's nuclear legacy consists of radioactive waste and spent fuels produced by these nuclear facilities, with 35 sites in the UK generating radioactive waste (NDA, 2011). According to the UK Radioactive Waste Inventory, the UK is accountable for 1620 m^3 of High Level Waste (HLW), 94000 m^3 of Intermediate Level Waste (ILW) and 66000 m^3 of Low Level Waste (LLW) (NDA 2011). The majority of the legacy waste can be found at Sellafield and Dounreay. Sellafield is the UK's largest nuclear

site, with its operations consisting of Mixed Oxide Fuel (MOX) fabrication, spent fuel reprocessing, and nuclear waste storage.

1.4. The Nuclear Fuel Cycle

One of the largest sources of radioactive waste originates from the nuclear fuel cycle (Wilson, 1996) (Figure 1). One of the stages of the nuclear fuel cycle, the reprocessing of spent fuel (post-reactor operation), was the major source of the liquid effluent which was discharged by BNFL into the Irish Sea.

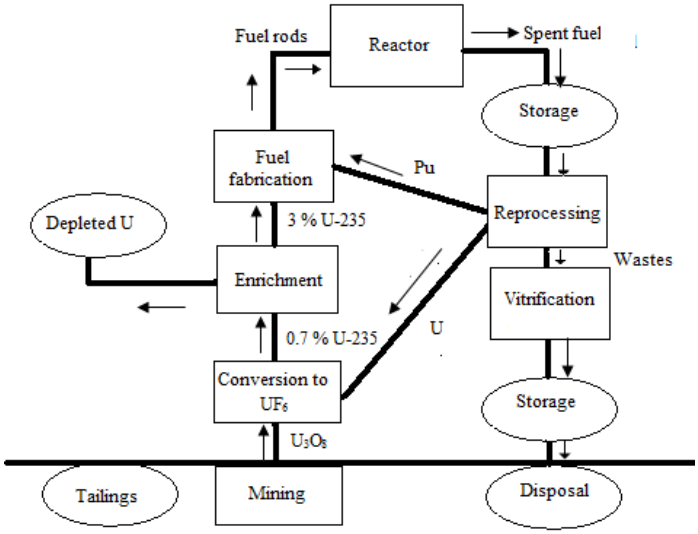

Figure 1. The nuclear fuel cycle

Indeed, radioactive wastes are produced at each stage of the nuclear fuel cycle and key processes such as U mining and milling and spent fuel reprocessing produce the largest amount of radioactive waste (Abdelouas, 2006). There are two types of nuclear fuel cycles in current operation: (i) an open fuel cycle which includes the eventual disposal of highly radioactive spent fuel; and (ii) a closed fuel cycle which

creates an intricate array of waste streams through reprocessing operations (Sharrad et al., 2011). The latter provides options for waste management, reducing radiotoxicity and the removal of fissile material from spent fuel etc.

1.4.1. Mining and Milling of Uranium Ore

Once a U deposit has been located it can be mined by leaching or extraction (Choppin et al., 2002). Canada, Australia, and Kazakhstan are the leading global suppliers of U ore, together producing over 50000 tonnes annually (Sharrad et al., 2011). The U ore retrieved from the deposit undergoes a series of chemical reactions and processes which include roasting and leaching with acid (Wilson, 1996). There are also many 'crushing' stages involved. During these processes U has varying oxidation states in order to reach the final milled product, U_3O_8 (also known as yellowcake), which contains 65-70 % U (Choppin et al., 2002). Solid waste from this process is known as 'mill tailings' and contains high levels of radium (Ra) which eventually decays to its daughter product, radon (Rn) gas. As Ra is a long-lived radionuclide there is an associated radiological risk, especially *via* inhalation, if adequate disposal of mill-tailings does not take place.

1.4.2. Purification and Fuel Fabrication

During milling operations, a large percentage of the 'waste' radionuclides (e.g. Th and Ra) are separated from U. However there are still impurities such as boron (B), cadmium (Cd) and molybdenum (Mo) which must be removed *via* a purification step (Wilson, 1996). In nature, U consists of three isotopes (^{234}U, ^{235}U, and ^{238}U), which contribute 0.055 %, 0.711 %, and 99.28 % of natural abundance, respectively (Choppin et al., 2002). As ^{238}U is not fissionable by thermal neutrons, the

concentration of ^{235}U must be increased in order to maintain a chain reaction in the core of the nuclear reactor. Early reactors such as the UK Magnox concept were specifically designed to use natural U, thus allowing the use of fuel having a natural isotopic composition (Ewing, 1999). Other reactors necessitate elevated levels of ^{235}U, most commonly requiring enrichment of ^{235}U to 3-5 % of atoms present. Two fundamental processes are used in commercial enrichment, (i) centrifugation, and (ii) gaseous diffusion (for further information see Wilson, 1996).

1.4.3. Reactor Operation

Enriched fuel is placed in the reactor as either U metal or UO_2 pellets which are usually encapsulated in metal rods within the core of the reactor (Chapman and McKinley, 1987). Nuclear power reactors are either fast or thermal, with the energy of the neutron flux being the underlying difference between both types. Currently nine out of the UK's ten existing nuclear power reactors are Advanced Gas Reactors (AGR) which use enriched fuels and stainless steel cladding. Further, these reactors use CO_2 to cool the high temperatures reached in the reactor core. The remaining UK nuclear reactor, Sizewell B, is a Pressurised Water Reactor (PWR). The cooling mechanism for PWR is *via* pressurised water and not CO_2 gas. In both cases the coolant absorbs heat from the core before leaving the reactor at temperature of 300 °C. The heat which is collected, is then used to drive a turbine and generate electricity. The UK Magnox reactors are currently offline, either being decommissioned or prepared for decommissioning.

1.4.4. Spent Fuel Reprocessing

Spent fuel is fuel which has been irradiated in a nuclear reactor and no longer has the ability to sustain a nuclear reaction. Due to the radioactivity of fissile U and the ingrowth of contaminants, spent fuel is thus removed from a nuclear reactor and stored to allow (i) decay heat to decrease, (ii) short-lived isotopes to decay, and (iii) to contain the radiation that is emitted from the fission products (Chapman and McKinley, 1987). The reprocessing of spent nuclear fuels is vital for their reuse and reduction of waste products. Further, solvent extraction is the dominant method used, which utilises the differing affinities of the actinides with ligands. The PUREX method is employed by the UK, and extracts Pu and U into a liquid phase, separating them from fission products and from each other. Post reprocessing, both Pu and U can be used to produce MOX fuels. This fuel has a greater concentration of fissile isotope (^{235}U), preventing the need for enrichment. The reprocessing of spent fuel is beneficial in reducing the amount of U required *via* mining, however the process itself generates large waste streams.

1.4.5. Radioactive Wastes and their Disposal

All steps in the nuclear fuel cycle produce wastes. These waste streams are categorised based on the level of radioactivity they contain. In the UK, HLW is defined as the intensely radioactive fission product stream that is derived from fuel reprocessing and requires constant cooling due to the decay heat it generates (Sharrad et al., 2011). This type of waste has a relatively small volume in comparison with other types of waste (ILW & LLW), however its activity comprises 95 % of the radioactivity in nuclear wastes causing the greatest difficulty for both

storage and disposal (NDA, 2011). ILW includes radioactively contaminated plant, equipment, and wastes from effluent treatment. LLW is the least radioactive and is defined as material which has a radioactive content not exceeding 4 GBq tonne^{-1} α or 12 GBq tonne^{-1} β/γ activity (Morris et al., 2011). LLW is mainly composed of PPE used in radioactive environments and wastes derived from decommissioning. These are disposed of by shallow burial at the national Low Level Waste Repository (LLWR) near Drigg, Cumbria.

Once the fuel has been stored for the requisite period it must be adequately disposed of. This can take place *via* direct disposal, which includes storage of the fuel in ponds to allow the decay of fission products and heat dissipation followed by complete disposal as waste (Ewing, 1999). This is the method currently favoured by the USA and Sweden. In contrast the open fuel cycle is currently preferred by Britain, France, and Japan.

In England and Wales, geological disposal has been chosen as the long-term management pathway for Higher Activity Wastes (HLW and ILW) (CoWRM, 2006). This involves both the placement and segregation of waste in a Geological Disposal Facility (GDF) that is built within a suitable rock formation to limit high doses of radioactivity from reaching the surface environment (Morris et al., 2011). The UK defines geological disposal as 'burial underground (200 – 1000 m) of radioactive waste in a purpose built facility with no intention to retrieve' (Hodgeson, 1999). Currently the USA operates the world's only GDF (The Waste Isolation Pilot Plant, (WIPP)) and in Europe, the Swedish, and Finnish GDF programmes are well advanced, having reached the stage of construction (Morris et al., 2011). In contrast, the UK GDF programme is still in its infancy and its implementation will require several decades of planning and construction.

1.5. Sellafield

The Sellafield Ltd. nuclear site is located on the Cumbrian coast. Here, the reprocessing facilities on site have released authorised LLW into the Irish Sea since operations began in the early 1950s, until termination of the effluent discharge took place in 1992 (Gray et al., 1995; Assinder et al., 1991). The liquid effluent discharged from the site contains purge water used in waste storage ponds and process liquors that originate from spent fuel reprocessing. The effluent contains actinide elements (e.g. Am, U, Pu, and Np) and fission products (e.g. ^{134}Cs, ^{137}Cs, ^{129}I, ^{90}Sr, and ^{99}Tc), which accumulate in mud patches in the Irish Sea causing the distribution of radionuclides in neighbouring estuaries (Marsden et al., 2006; Morris, 1996; Kershaw et al., 1986; Livens and Sajih, 2010). Due to their various half-lives, there has always been a significant interest to characterise the behaviour of these radionuclides in the environment and to assess any potential risks they may have on ecosystems and the neighbouring population.

1.5.1. Operational History of Sellafield

The 1940s saw the birth of Sellafield as an ordnance manufacturing plant. The construction of two air-cooled, Pu-producing reactors (Windscale Piles) signified the start of the UK nuclear efforts to support the country's ongoing military agenda. Until the mid 1950s, the sole aim of Sellafield was to supply weapons to the Ministry of Defence to strengthen the military programme. After several years of planning and research, the world's first commercial nuclear reactor (Calder Hall) began generating electricity at the Sellafield site in 1957. By the 1960s, nuclear power generation was more profitable to large energy companies rather than research and military ventures. As a result, in 1963, the Windscale Advanced Gas Cooled

Reactor (WAGR) prototype began operating (NDA 2011). The Magnox Reprocessing Plant was introduced shortly after in 1964, receiving spent fuel from all UK Magnox reactors and converting them into products which would be suitable for long-term storage.

Over the years Sellafield has changed from a nuclear facility focusing on product operations to one which is centred on the decommissioning of Windscale and Calder Hall reactors, including the storage and reprocessing of spent fuel at Magnox and THORP. Currently there are four operations which take place within the 262 hectares of Sellafield, these are: waste management, reprocessing, spent fuel receipt, and decommissioning. Over time, Sellafield has become one of the largest contributors of anthropogenic radionuclides to the environment *via* the nuclear fuel cycle. This cycle has historically generated vast amounts of nuclear power, unfortunately yielding large waste streams which are associated with the fission process. The leakage or inadequate disposal of radioactive waste coupled with authorised effluent discharges into the Irish Sea from 1952-1992, has resulted in the radioactive contamination of the marine and coastal environment surrounding Sellafield.

1.6. Radionuclides in the Environment

Various nuclear events/processes can result in radioactive material being released into the environment. Typical sources of radioactivity are from nuclear facilities, nuclear weapons testing, and nuclear accidents (UNSCEAR, 2000). Atmospheric nuclear weapons testing is a major source of α-emitters in the environment causing global deposition of over 14.8 x 10^{15} Bq of ^{239,240}Pu between 1944 to 1963 (Bowen et al., 1980; Scholkovitz, 1983). The IAEA have estimated that the majority of the 16

x 10^5 Bq ^{239,240}Pu released by nuclear weapons has become deposited in the marine sediments. Nuclear accidents (e.g. The Windscale Fire, U.K, 1957 and Chernobyl, Ukraine, 1986) also introduced high levels of radionuclides into the atmosphere.

1.6.1. Authorised Sellafield Discharges

The authorised discharge of radioactive effluents from the reprocessing plant at Sellafield has resulted in significant contamination of the Irish Sea. The direct release of radioactive waste to the marine environment has taken place since operations commenced at the site in 1952. Discharge to the Irish Sea occurred *via* pipelines which extended 2.5 km from the high water mark and ended 20 m below the surface of the water (Gray et al., 1995).

Low level liquid effluents originated from various sites at Sellafield, most commonly from separation extraction processes which produce liquors. Reprocessing was stopped temporarily in 1974 resulting in the increased residence time of Magnox fuel in storage ponds. As a result there was an increase in the concentration of soluble radionuclides in the cooling pond waters. Thus between 1974-1978 ^{137}Cs reached maximum discharge values (Figure 2). The decrease in discharge activity also occurred after the 1980s due to a number of significant measurements which were implemented by BNFL. Here, the discharge of medium-active concentrate was terminated and fuel storage pond water was purified and treated by passing through several sand filters and clinoptilolite ion exchangers (Gray et al., 1995). The authorised discharge of LLW into the Irish Sea was terminated in 1992. Annual discharge data for ^{241}Am and total Pu (the isotopes ^{238} Pu, ^{239} Pu and ^{240}Pu) also reached a maximum in the 1970s due to the increase in throughputs and processing

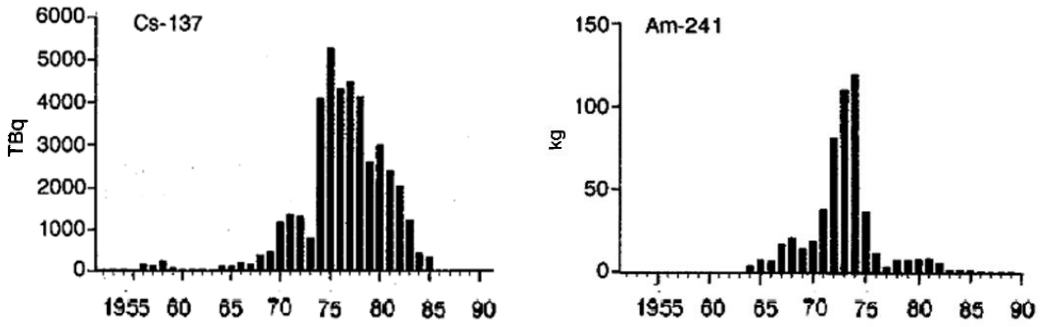

Figure 2. Discharge of ^{137}Cs (TBq) and ^{241}Am (kg) in liquid effluent from Sellafield between 1955-1990 (taken from Kershaw et al., 1992).

of residues (Figures 2 and 3). The implementation of a flocculation precipitation treatment facility from the mid 1970s, coupled with the commissioning of the Salt Evaporator in 1985 caused the activity of these discharges to decrease (Gray et al., 1995).

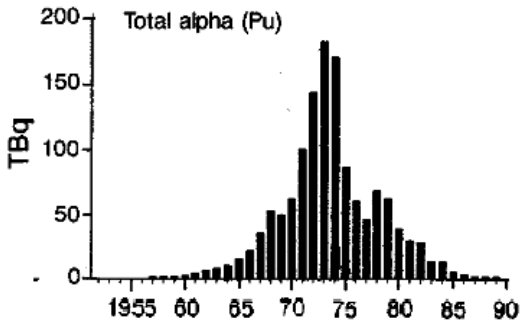

Figure 3. Discharge of ^{238,239,240}Pu (TBq) in liquid effluent from Sellafield between 1955-1990 (taken from Kershaw et al., 1992).

1.7. The Chemistry of Select Actinides and Fission Products in Sellafield Effluents

The actinides are a series of fifteen elements consisting of atomic numbers 89 (actinium, Ac) to 103 (lawrencium, Lr). The chemical properties of actinides and their heavier counterparts, the transactinide elements, are governed by their outermost electronic configuration. Going from Ac to Lr, the actinide series sequentially fills the 5f atomic sub-shell as an electron is added. Extensive research into environmental samples taken from the area surrounding Sellafield show the presence of several long-lived actinides e.g. ^{238}Pu, ^{239,240}Pu, ^{241}Am and several fission products ^{137}Cs, ^{90}Sr (Assinder et al., 1991; Aston and Stanners, 1982; Kershaw et al., 1984).

1.7.1. Plutonium

Plutonium (atomic number 94) is a transuranic element. In 1940 Pu was discovered during fission experiments conducted by Seaborg and co-workers at Berkeley, USA (Seaborg et al., 1946). Here, they found that bombarding ^{238}U with deuterons resulted in the fission product ^{238}Np (Equation 1); this would eventually β-decay to produce ^{238}Pu (Equation 2). The short half life of this Pu isotope in tracer studies allowed Seaborg and co-workers to elucidate the presence of other Pu isotopes.

$$^{238}\mathrm{U} + {}^{2}\mathrm{H} \longrightarrow {}^{238}\mathrm{Np} + 2\,{}^{1}\mathrm{n} \quad \text{(Equation 1)}$$

$$^{238}\mathrm{Np} \xrightarrow{\beta^-} {}^{238}\mathrm{Pu} \quad \text{(Equation 2)}$$

In 1941, a Pu isotope of major importance (^{239}Pu) was discovered. Here, bombardment of ^{238}U with neutrons produced ^{239}U which decayed to ^{239}Np and to ^{239}Pu (Equation 3). In nuclear reactors, higher mass plutonium isotopes are formed *via* consecutive neutron capture reactions (Equation 4).

$$^{238}U + {}^{1}n \longrightarrow {}^{239}U + \gamma \qquad \text{(Equation 3)}$$

$$^{239}U \xrightarrow{\beta^-} {}^{239}Np \xrightarrow{\beta^-} {}^{239}Pu \qquad \text{(Equation 4)}$$

The majority of Pu isotopes found in the environment are of an anthropogenic nature, with nuclear weapons tests being the main source for their existence. ^{238}Pu is a fissile isotope and is produced in nuclear reactors from the decay path of ^{238} Np. The heavier Pu isotope, ^{239}Pu, is used in energy production and nuclear weapons (Choppin et al., 2002; Sajih, 2006), whilst ^{241}Pu is a fissile isotope and is significant as it decays to the α-emitting ^{241}Am. The nuclear properties of the Pu isotopes are shown in Table 1. Plutonium is an important radionuclide from an ecological perspective as all its four isotopes are present in the environment in appreciable activities.

The simultaneous presence of one or more oxidation states in solution makes it difficult to predict actinide environmental behaviour with changes in E_h, pH, ligand concentration etc. (Choppin, 2006). Plutonium can be found in a range of oxidation states; namely, from +3 to +5. Plutonium(III) is prevalent in reducing waters and in the presence of elevated organics, which can lead to complexation with humic substances. Regardless of the geographical location, it has been well established that

Table 1. Properties of environmentally significant Pu isotopes

Pu isotope	Half-Life (y)	Route of production	Decay Path	Decay energy (MeV)
^{238}Pu	87.75	^{242}Cm, ^{238}Np daughter	α	5.499, 5.257
^{239}Pu	24390	^{239}Np daughter, n capture	α	5.155, 5.143
^{240}Pu	6537	Multiple n capture	α	5.188, 5.124
^{241}Pu	14.89	Multiple n capture	β	0.02

the pentavalent species PuO_2^+ dominates in waters close to the coastline or surface (Choppin and Wong, 1998). In contrast the tetravalent Pu^{4+} species is found more readily in open waters alongside the oxidised +5 form. Further, decreased solubility and mobility is found for the lower oxidation states +3 and +4 in marine environments, as the high charge density of the species is able to hydrolyse water forming a Pu precipitate e.g. $[Pu(OH)_3]$ or $[Pu(OH)_4]$. Conversely the PuO_2^+ species does not hydrolyse water as it has low charge density, thus it is souble and mobile in a water column. The difference in behaviour of Pu isotopes in the Irish Sea, enables them to be transported from the pipeline to the saltmarsh by particulate and solution phases. The relatively long half-lives coupled with the toxicity of the Pu isotopes also make them a potential radioactive hazard if they are present in the environment especially, in public areas (e.g. Ravenglass, UK).

1.7.2. Americium

Americium (atomic number 95) is formed from the decay of ^{241}Pu which originates from multiple neutron captures of ^{239}Pu (Equation 5). The most significant isotopes of Am are, ^{241}Am and ^{243}Am due to their long half-lives of 433 and 7380 years, respectively (Choppin et al., 2002). The isotope ^{241}Am is a α and γ-emitter, with characteristic α-particle energies at 5.44 MeV and 5.49 MeV, and a characteristic γ-energy at 59.5 keV (Browne and Firestone, 1986). Both of these isotopes are produced in commercial nuclear reactors.

$$^{239}\text{Pu}\ (n, \gamma)\ ^{240}\text{Pu}\ (n, \gamma)\ ^{241}\text{Pu} \xrightarrow{-\beta^-} {}^{241}\text{Am} \qquad \text{(Equation 5)}$$

The only stable oxidation state of Am in environmental systems is Am^{3+}, hence it is not a redox active radionuclide. In solution, the high charge density of Am^{3+} causes it to hydrolyse water forming a precipitate, $[Am(OH)_3]$, thus reducing its mobility in marine environments. Consequently the dominant transport mechanism for Am from the Sellafield pipeline is suggested to be *via* association to particulates (similar to Pu^{4+}). Using discharge records from Sellafield, approximately 27 % of the total ^{241}Am content in the Irish Sea in 1980 originated from the decay of ^{241}Pu (Day and Cross, 1981). As previously mentioned ^{241}Pu has a short life (14.4 years) and consequently after five half-lives have elapsed, more than 95 % of ^{241}Pu has decayed to ^{241}Am (Gray et al., 1995). There is also significant indirect contribution of ^{241}Am from weapons testing as it leads to the release of the parent nuclide ^{241}Pu into the environment.

1.7.3. Caesium

The isotope ^{137}Cs is a fission product and has a half life of 30 years. Nuclear weapons testing and discharges from nuclear facilities are the principal sources of ^{137} Cs in the environment. A significant release of the alkali metal into the northern hemisphere occurred during the Chernobyl accident, 1986 (Ilyin et al., 1990). Further, the reprocessing plant at Sellafield released a total ^{137}Cs activity of 41 PBq into the Irish Sea between 1952-1998 (Smith, 2011). Caesium exists as a monovalent cation in environmental systems. Interestingly, its behaviour differs between open water and that of sediments. The monovalent Cs species has a low charge density; hence in solution it cannot withdraw electron density from the surrounding water molecules, thus it is not readily hydrolysed. As a result, the species is highly soluble leading to enhanced mobility, with Cs forming an aqueous complex. In sediments Cs is incorporated into the crystal structure of minerals as it is exchanged for K in illitic clay minerals, reducing its mobility significantly. Hence it can be observed that the processes which take place in the marine and coastal systems have an effect on radionuclide behaviour.

1.8. Biogeochemistry of the Natural Environment

In order to understand radionuclide behaviour in environmental media (e.g. soil, waters, and sediment), it is essential to recognise the mineral-microbe interface that is present in natural systems. Biogeochemical processes in the subsurface which involve the microbial and mineral constituents of sediments and rocks have a major affect on the bioavailability, speciation, mobility, and ecotoxicity of radionuclides in environmental systems (van Hullebusch et al., 2005). Key geochemical processes

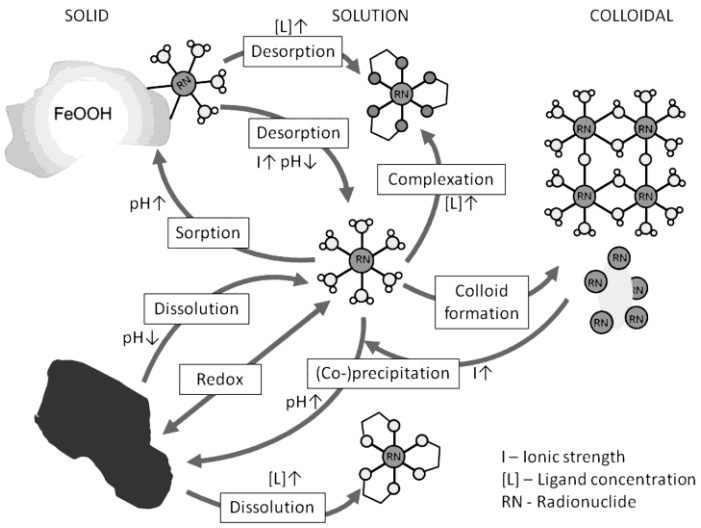

Figure 4. Key geochemical processes that influence the speciation of radionuclides in the environment (Brookshaw et al., 2012).

which influence radionuclide behaviour are: sorption, co-precipitation, dissolution, complexation, redox reactions, microbial interactions, and colloidal formation (Figure 4) (Brookshaw et al., 2012).

1.8.1. Sorption

The sorption of a particular radionuclide to the surface of a mineral in the environment can reduce radionuclide mobility. Once the radionuclide is in contact with the mineral, it will redistribute between the solid and aqueous phases. The radionuclide can interact with the mineral surface *via* three types of sorption (chemisorption, physisorption and ion exchange). During chemisorption the radionuclide forms a strong covalent bond to the radionuclide and the mineral surface, producing an inner sphere complex. Physisorption involves weak Van der Waals forces between the radionuclide and the mineral surface resulting in an outer

sphere complex. Physisorption interactions are weak in nature and thus there is a greater likelihood of the radionuclide being desorbed from the mineral surface. The mechanism for ion-exchange involves the substitution of a radionuclide ion with an ion from the mineral structure (e.g. Cs^+ replacing K^+ in layered clay arrangements). The optimum pH for radionuclide sorption to the majority of environmentally relevant minerals is at neutral pH. Fluctuations in pH can lower the interactions/ electrostatic attractions between radionuclides and minerals thereby reducing effective sorption.

1.8.2. Incorporation/Precipitation

The effective sorption of radionuclides to mineral surfaces can act as a precursor for co-precipitation or incorporation into mineral lattices in some cases. Radionuclides which are present in solution can be sequestered by being co-precipitated with a mineral phase (e.g. calcite) and incorporated into its structure (Brookshaw et al., 2012). Once the radionuclide has incorporated into the crystal structure of a mineral it is irreversibly bound, unless the structure of the mineral is broken down. Precipitation reactions are most likely to occur when a chemical non-equilibrium exists, for example, near the Sellafield LLW pipeline.

1.8.3. Redox Reactions

The concept of the redox cascade is important for redox sensitive radionuclides (those which have stable, accessible oxidation states) such as U, Pu, and Np. For these radionuclides sorption reactions are readily coupled with a surface mediated oxidation or reduction between the radionuclide and structural groups within, or that are adsorbed onto minerals. For example, the redox potential between Pu^{6+} and Pu^{5+}

is small and thus an increase in microbial activity may cause the reduction of Pu^{6+} to Pu^{5+}, causing increased dissolution of Pu (Brookshaw et al., 2012). The redox reactivity of a mineral surface is dependent on the speciation of the redox sensitive species and on whether they are sorbed or structurally bound; for example, Fe^{2+} is known as a strong reducing agent in subsurface environments (Charlet et al., 1998). It has been shown that a mixed Fe^{2+}- Fe^{3+} phase can immobilise as much as 99.8 % Tc(VII) from solution, predominantly *via* reduction (Pepper et al., 2003). This is important as Fe is an element present in natural sediments and thus it may have an effect on radionuclide sequestration.

1.8.4. Bioturbation

The distribution of radionuclides in certain systems can be controlled by fauna. The term bioturbation describes all faunal transport activities that directly or indirectly disturb the substratum (Aller and Aller 1992; Forster et al., 1995). In reality, bioturbation encompasses two types of activities, namely particle reworking (direct movement of particles by animals) and burrow ventilation (direct movement of water) (Kristensen et al., 2012). This is a diffusive like process, with the strength of the transport being represented by a biodiffusivity parameter (D_B). The process of bioturbation is important in understanding the fate of radionuclides in the Irish Sea. For example, for certain radionuclides (e.g. Cs) that have been deposited in the Irish Sea mud patch, the burrowing motion of polycheates causes significant mixing and particle re-working of the sediments, re-suspending radionuclides into the water column and augmenting off-shore transport (Forster et al.,1995). The extent of bioturbation on the mixing of sediments varies from one environmental system to another. For cores taken from a saltmarsh environment, it has been found that

bioturbation only takes place significantly in the top few centimetres of the sediment (Hetherington, 1978; Libes, 1992). In contrast bioturbation has been shown to cause redistribution of radionuclides to a depth of 1.4 m in core samples taken from the Irish Sea (Kershaw et al., 1984).

1.8.5. Microbial Activity

The geochemistry of estuarine sediments is reflective of both the composition of the material which is originally deposited at the site, and the various physical, biological, and chemical processes which affect this material post-deposition. This process results in the alteration of a rock's original mineralogy and texture and is known as early diagenesis. The majority of diagenetic reactions have been recognised to be microbially-mediated redox reactions which result in the remineralisation of organic matter. Organic diagenesis is the process whereby organic matter is oxidised, coupled to the reduction of a Terminal Electron Acceptor (TEA) that yields the greatest free energy change per mol of carbon oxidised (Froelich et al, 1979). Microorganisms utilise this process to fuel their metabolic pathways. This transport of electrons has an associated net free energy gain, and is known as the standard Gibbs free energy ($\Delta G°$). Microbial species in the environment will always seek to maximise the $\Delta G°$ of the redox reaction taking place.

For an oxic system, O_2 yields the highest Gibbs free energy per mol of carbon oxidised and consequently is the primary electron acceptor used under these condition (Froelich et al., 1979). As oxidants are consumed, the TEAs of a system are altered. A sequential system is in place and as one TEA becomes depleted, microorganisms will proceed to the next most efficient (most energy producing) oxidant in order to meet their energy demands. This order of usage of oxidants is

known as the redox cascade and is the typical order in which microorganisms will exploit TEAs at the subsurface. The order of the redox cascade follows as O_2, NO_3^-, NO_2^-, $Mn^{4+/3+}$, Fe^{3+}, and SO_4^{2-} after which methanogenesis can take place (Figure 5).

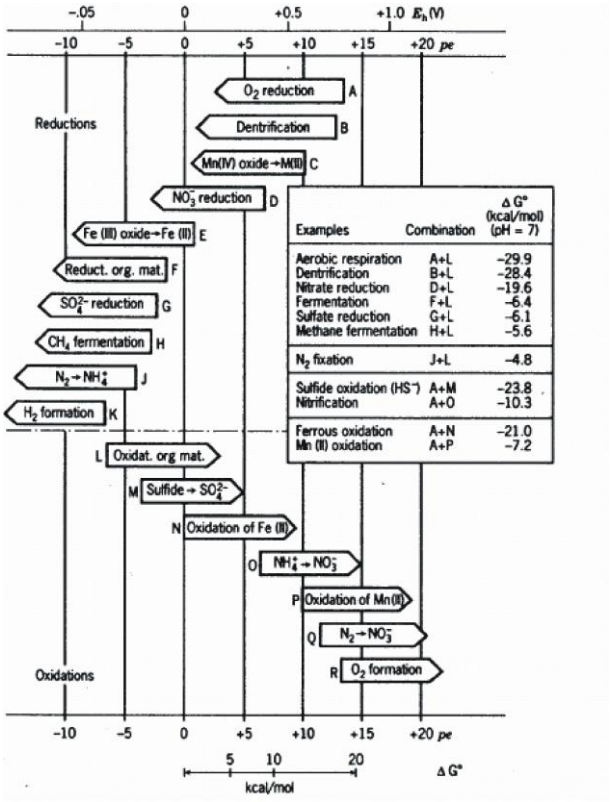

Figure 5. The microbially-mediated redox cascade, showing the net free energy gain associated with each electron acceptor per half reaction, in kcal per mol of carbon oxidised at pH 7 (taken from Stumm and Morgan, 1996).

As O_2 levels become depleted, organic matter is successively broken down. As less oxidant remains, the substratum changes to a more anoxic, reducing environment. In the absence of O_2, redox sensitive radionuclides such as UO_2^{2-} and TcO_4^- present in contaminated systems are also exploited as TEAs by microorganisms, causing them to be reduced. Most importantly, this reduction will cause the oxidation state of the radionuclide to alter, causing the mobility of the contaminant to change in the

environment. Metabolic activities in environments depleted of O_2 are less energetically favourable, in comparison to aerobic respiration. Facultative anaerobes are capable of both aerobic respiration and anaerobic respiration, switching to the latter when O_2 is unavailable. These microorganisms reside in the suboxic zone, regulating their metabolism to utilise O_2 as the principal oxidising agent when it is available (Dolfing and Tiedje, 1988).

1.9. Mechanism of Radionuclide Transportation

Sellafield effluent containing fission products and actinides has been released into the Irish Sea *via* pipeline discharge. The aim of the controlled release of LLW was for the effluents to be discharged to the Irish Sea which would then subsequently flow outwards into the Atlantic Ocean. However, it appears that as the LLW emerged into the marine environment, a proportion of it precipitated within the local marine environment causing it to flocculate and sediment. The transuranic elements, predominantly Pu, were lost from the effluent within 12 hours of discharge and as a result 95 % of Pu and the majority of Np and Am is estimated to have become associated with sediment on the Irish Sea floor (Hetherington et al., 1978).

As shown in Figure 6, the dominant sediment type surrounding the pipeline outlet is a belt of fine-grained, mud-like particulates. The muddy sediments are located in two main areas: a belt of muddy sands and muds parallel to the Cumbrian coast extending into Liverpool Bay, and across the mouth of the Solway Firth to Wigtown Bay (Kershaw et al., 1992). Radionuclides that are deposited here tend to strongly associate with the fine-grained sediment. As discussed previously the fauna (polycheates) re-work the contaminants causing them to be redistributed into the water column. The radionuclides are then transported to surrounding estuaries and

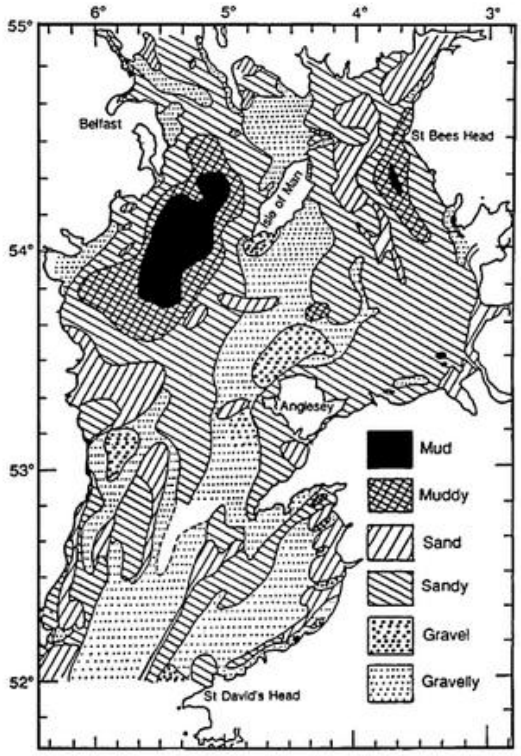

Figure 6. Distribution of sediment types in the Irish Sea, in the vicinity of the Sellafield site by grain size (Pantin, 1991).

neighbouring regions *via* open marine (both surface and current) and tidal currents. The Ravenglass saltmarsh is a sink which is controlled by tidal currents and consequently it receives colloidal and particulate radioactive matter from the Irish Sea (Choppin, 1994). As the radionuclides approach coastal regions they are deposited on the shore during high tide. As these events are repeated a layered profile is imbued in the estuarine sediments illustrating the discharge history that has occurred since 1952 (Gray et al., 1995). Sediments at the bottom of the profile contain waste radionuclides from around the mid 1950s. In comparison sediments on the top of the profile will have been deposited more recently and contain radionuclides from around the mid-1970s onwards. The biological, physical, and

chemical processes which take place in natural environments (in both the mud-patch and saltmarsh) can affect the distribution and migration of radionuclides. Post depositional mixing can also alter a sediment profile. Hence it is important to understand such processes.

1.10. Project Aims

This study builds on work carried out by Morris (1996) and Marsden et al., (2006) who examined the fate of Sellafield borne radionuclides in the Ravenglass Estuary during the 1990's and early 2000's. Overall it seeks to provide contemporary insight into the activities and distribution of ^{137}Cs, ^{241}Am, ^{238}Pu, and ^{239,240}Pu in the estuaries subsurface. Further, many studies have acknowledged that the accumulation of anthropogenic radionuclides does take place at intertidal sites in the vicinity of Sellafield (Assinder et al., 1991; Aston and Stanners, 1982; Kershaw et al., 1984), but most importantly it is the assessment of potential movement of these radionuclides in comparison with previous studies that is key here. Furthermore, this will provide a greater understanding of the variance in radionuclide distribution with time. Importantly, the Ravenglass area is a public location, it is not within the Sellafield grounds and thus it is vital to consistently monitor the levels and distribution of contamination present. If the radionuclides were to reach the surface sediments or move to another site, there may be undesirable radiological consequences for local ecosystems or populations.

In summary, the aims of the project are:

1. To quantify the concentration and distribution of ^{137}Cs, ^{241}Am, ^{238}Pu and ^{239,240}Pu in a sediment core taken from the Ravenglass saltmarsh;

2. To relate the radionuclide distribution to the Sellafield authorised discharge record;
3. To relate the radionuclide distribution (mainly Pu) to Fe and Mn geochemistry;
4. To compare results from previous findings published in the literature thus determining any potential temporal remobilisation or depositional trends.

Chapter 2
Materials and Methods

2.1. Sample Collection

The location of the sampling site in the Ravenglass saltmarsh was the same as that used in previous studies, e.g. Hursthouse and Livens, 1993 and Hamilton and Clarke, 1984. The sediment accumulation rate for the salt marsh is estimated to be ~ 4 mm yr^{-1} (Kelly and Emptage, 1992) and thus a core of approximately 25 cm depth would be sufficient to encompass the entirety of the Sellafield discharge history. Reflecting this, a pit was dug at the chosen site, (Figure 7) and one face cleaned off and made vertical.

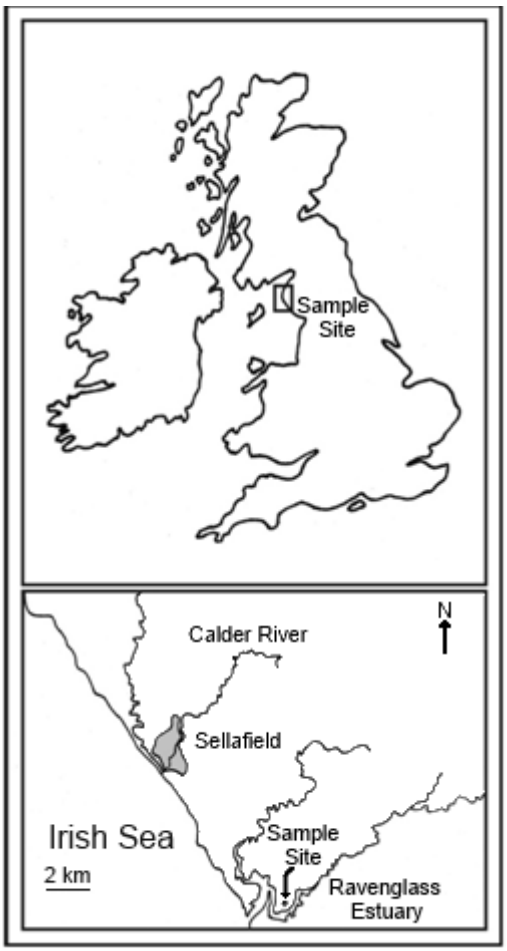

Figure 7. Sampling site at the Ravenglass saltmarsh.

A block of sediment (25.5 cm deep x 15 cm x 15 cm) was cut out with a spade and placed on a plastic sheet; thereafter the sediment block was sectioned with a sharp knife into 17 equal slices, with each quotient having a depth of 1.5 cm. Each section was sealed into a zip-lock PVC bag and returned to the laboratory. The sediments were wet-sieved through a 2 mm mesh to remove any large solids and then air dried. The sieved, dried sediment was ground to a talc-like consistency on a Fritsch agate ball grinder. The resulting sediment was then weighed to approximately 20 g and 1 g fractions (20 g fraction for analysis *via* γ-spectroscopy and 1 g fraction for analysis *via* α-spectroscopy.)

2.2. Major and Minor elemental analysis

The major and minor elemental concentrations of the sediment samples were determined by X-Ray Fluorescence (XRF) spectrometry. X-Ray Fluorescence is a non-destructive elemental characterisation technique that can be used for powdered, solid, or liquid samples. The XRF spectrometer measures the individual component wavelengths of fluorescent X-ray emission produced by a sample that is irradiated with incoming X-rays. In this project, measurement was conducted on pressed powder pellets. Here, homogenised sediment samples (12 g) were mixed with 3 g of powdered wax binder. After homogenisation the sample/wax mix was pressed into a pellet for analysis. Analysis was conducted on an Axios Sequential X-Ray Fluorescence Spectrometer using a standardless analysis programme with IQ^{+}. Data (major elements) was then oxide normalised.

The concentration of 'reactive' Fe in the dried sediments was quantified using a standard extraction technique (Viollier et al., 2000). Here, 0.1 g of the sieved, dry sample was weighed, and added to a centrifuge tube. 5 mL of 0.5 M HCI was added

and left to digest for 60 minutes. The sample was then centrifuged at 4000 rpm for 3 minutes. Thereafter to each cuvette for sample measurement; 900 µl of DI, 100 µl of Ferrozine solution, 100 µl of aqueous Fe buffer, 200 µl of HA-HCI and 100 µl of sample was added. For the blank sample the 100 µl of sample was replaced with 100 µl of DI. Additionally five standards were made at the following concentrations: 20, 40, 100, 200, and 400 (µM). For the cuvette containing the standards the 100 µl of sample was replaced with 100 µl of solution from the corresponding standard. After all aqueous additions were complete, each cuvette was covered with parafilm and mixed by inversion. The samples were then measured against the blank and the standards on a PG Instruments T60 UV-Vis spectrophotometer at 562 nm (visible region). Calibration using the known standards gave an R^2 value > 0.972.

2.3. Americium and Caesium Detection

Americium-241 is formed by the consecutive neutron absorption by Pu in neutron reactors and nuclear weapons testing, which is then followed by β-decay. As ^{241}Am decays to ^{237}Np the nucleus emits both high-energy α-radiation and low-energy γ-rays. The nuclear fission product ^{137}Cs is formed when U and Pu in nuclear fuel capture thermal neutrons and undergo fission. Radioactive Cs decays *via* emission of a β-particle and γ-rays producing, ^{137m}Ba. Both of these isotopes emit γ-rays during their decay path. Due to the ease of sample preparation and the efficiency of the detector, γ-spectroscopy was chosen as the technique to quantify ^{241}Am and ^{137}Cs activities in the Ravenglass sediment samples.

2.3.1. Gamma Spectroscopy Theory

The radiometric technique of γ-spectroscopy utilises the penetration of electromagnetic radiation. The high energy penetration gives a count rate for the sample which quantifies the amount of activity present;

$$\text{Count rate} = \frac{\text{No. of counts}}{\text{Counting time}}$$

The emission of a γ-ray, at a specific energy is reflective of the isotope present, which is extremely useful in characterising radionuclides. The sample does not require chemical treatment prior to counting as γ-radiation is penetrating. Additionally this minimises any potential risk from cross-contamination.

Semiconductor detectors such as Si(Li) or lithium drift germanium Ge(Li) have been predominantly used for γ-spectroscopy measurements of environmental samples due to their high energy resolution (Eberth and Simpson, 2008). A band structure is present in the semiconductor crystal, with the band gap being smaller for Ge than Si. The movement of γ-photons creates enough energy to displace electrons from the valence band to the conduction band, creating an electron-hole pair. The probability that an electron will jump into the conduction band is dependent on temperature and small band gaps such as those in Ge crystals can lead to electrons having enough energy (E_g) to cross the band gap- even at room temperature. As a result these semiconductor crystals are constantly cooled to 77 K with liquid nitrogen to maximise resolution (Garnir et al., 2008).

When an electric field is applied, the hole and the electron migrate through the crystal to produce an electrical signal which is transported to the counting equipment. The signal is converted to a digital form and stored in a Multi Channel Analyser

(MCA) to produce the spectrum (Ehmann and Vance, 1991). Software such as Maestro can be used to the view and analyse the resulting spectrum.

Small Ge detectors or Si(Li) detectors are used for the measurement of low energy γ-rays and X-rays (< 100 keV) whilst larger Ge detectors are more suited for high energy γ-rays (Hou and Roos, 2008). The detection limit of γ-spectrometry (~ 50 mBq) is a few orders of magnitude higher than both α-spectrometry and β-counting, however this is largely dependent on the radionuclide of interest, interfering radionuclides, and the shielding by the detector (Hou and Roos, 2008). Conversely, the counting efficiency of the technique is relatively low (~ 10 % for absolute counting efficiency), however this is dependent on a number of variables: γ-ray energy, size of the Si or Ge crystal and distance from the source to the detector.

2.3.2. Gamma Spectroscopy Procedure and Analysis

In this study, the sieved sediment was sealed for 30 days to prevent exposure of the sample to moisture and to allow a route of analysis *via* γ-spectroscopy. Samples were sealed and stored for one month prior to measurement to enable a radioactive equilibrium to be attained between ^{226}Ra and its short lived daughter, ^{222}Rn (Rn gas). Prior to counting the samples, a γ-standard was made and analysed. This permitted the collection of both qualitative (the nuclei present) and quantitative (concentration) data. The standard was made by taking ~ 20.0 g of sediment (sample taken at 21-22.5 cm) and mixing with copious amounts of ethanol to form a slurry. The slurry was allowed to settle, after which the top layer of ethanol was spiked with 500 Bq of ^{210}Pb and 100 Bq of ^{226}Ra, ^{241}Am, and ^{137}Cs. The mixture was then homogenised gently and placed on a warm sand bath until dry (i.e. all the ethanol had evaporated). The standard was then sealed for 30 days prior to counting *via* γ-spectroscopy. Both

the standard and samples were counted for 24 hours on a Ge(Li) CANBERRA γ- spectrometer. Both ^{137}Cs and ^{241}Am can be detected at relatively low levels using the 661.6 keV (85 % abundance) and 59.5 keV (36 % abundance) γ-emission line, respectively. The net area or counts of the peaks at these respective energies were analysed, allowing quantification of the activity present in the sample for each isotope. The difference between the net area of peaks at 661.6 keV and 59.5 keV for the γ-standard and that of the background provide information on the detector efficiency.

2.4. Plutonium Detection

Plutonium isotopes of anthropogenic origin (^{238}Pu, ^{239}Pu and ^{240}Pu) are present in the environment due to nuclear processes. The quantification of these long-lived α-emitting isotopes can be detected using α-spectroscopy.

2.4.1. Alpha Spectroscopy Theory

Alpha spectroscopy is a common, analytical tool for measuring trace level, α-emitting radionuclides in environmental samples. The counting method utilises the α-decay of the nucleus of the radioisotope which results in the emission of a respective α-particle with a charge of +2. These α-particles bombard the Si/Ge detector with characteristic energies. Signal processing similar to that used in γ- spectroscopy results in the formation of the characteristic energy peaks.

The application of α-spectroscopy requires the fulfilment of certain criteria; namely the elimination of other α-emitters from the sample whilst ensuring that all samples are thin in nature (Tome et al., 2002). As a result, samples must be chemically

separated prior to being counted. Failure to prepare a sample which has a thickness negligible to that of α-particles will result in loss of resolution, as alpha particles will scatter within the sample (De Regge and Boden, 1984). This is due to the non-penetrating nature of α-particles. Prior to counting on the α-spectrometer, a stainless steel planchette must be prepared which is coated with a layer of Pu. This is achieved by electrodeposition after the separation of Pu has been carried out.

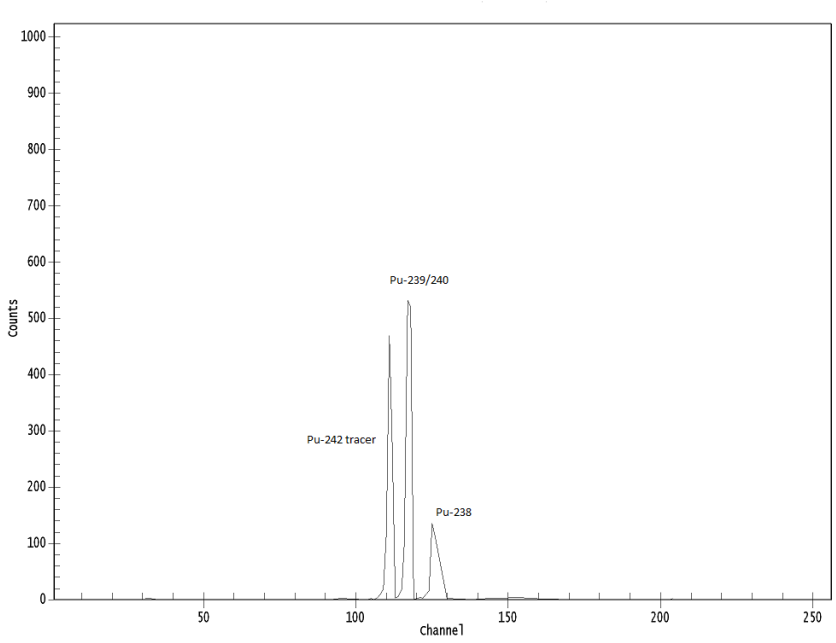

Figure 8. A typical environmental Pu α-spectrum.

The radiometric method has moderate efficiency, and this coupled with low background results in high sensitivity. Due to the resolution limitations of an α-spectrometer it can be difficult to distinguish peaks with similar energy. The isotopes ^{239}Pu and ^{240}Pu have similar α-energies (5.157 MeV and 5.168 MeV) and consequently produce a single peak in the α-spectrum (Figure 8). As a result their activity is commonly represented as the isotopic ratio ^{239}Pu/^{240}Pu, which can also be seen in previous literature and discharge histories. The use of a ^{242}Pu tracer during

chemical separation enables radiochemical yields to be determined. The area of the specific peak in the spectrum, or the number of counts is relative to the isotopic activity. The unknown activity can then be calculated using a simple formula (where A is the activity);

$$\text{A (sample)} = \frac{\text{Counts (sample)}}{\text{Counts (tracer)}} \times \text{A (tracer)}$$

2.4.2. Ion Exchange Resin

There are two types of ion exchange resins used for separating radionuclides: (i) cation and (ii) anion exchange resins. Cation exchange resins withdraw any cations from the solution whilst anionic resins do the same but with anions. The resin contains a network of small spheres made of organic polymers which have ionic pores within them. The sample solution is passed through the ion exchange column which allows an ion in a particular oxidation state to be retained on the resin bed. For the separation of Pu from the sediment, an anionic resin is used as Pu is retained on the complex as $[PuCl_6]^{2-}$. Thereafter, introduction of a new solution into the column changes the oxidation state of the ion (by reduction/oxidation) causing the radionuclide to be eluted from the sample. As various solutions cause the elution of different radionuclides, theoretically Pu, Am, and U can be separated from each other and from the same sample solution. However there are other factors which determine the productivity of this (for example, the amount of starting sediment used).

Adsorption of Pu^{4+} onto the resin is achieved with 9 M HCI followed by elution of stable Fe^{3+} by 8M HNO_3 (Talvitie, 1971). Plutonium is then eluted from the column by reducing Pu^{4+} to Pu^{3+} through the use of an appropriate reducing agent (e.g. HI)

(Sajih, 2006). Complexation of the Pu^{4+} can occur with both HNO_3 and HCI. Stepwise complexation occurs as the concentration of Cl^- ions is increased and Pu will be in the form $[PuCl_5]^-$ and $[PuCl_6]^{2-}$ (Cleveland, 1979). 9 M HCl was chosen as the preferred method of complexation in this project as it permits faster reaction rates, which inturn ensures adsorption of Pu^{4+} onto the resin (Talvitie, 1971).

2.4.3. Alpha Spectroscopy Procedure and Analysis

2.4.3.1. Chemical Separation of Plutonium

Prior to analysing a desired isotope *via* radiometric techniques such as α-spectroscopy, the radionuclide must be chemically separated from other minor and major isotopes present in the sample and also from the organic phase present. During the chemical separation procedure, the various α and β-emitting radionuclides are eluted at various stages. To determine the chemical yield, a known amount of tracer that has the same chemical behaviour as the desired radionuclide but is not present in the sample, is added prior to the sample entering the column. An anion exchange column is then used to chemically separate the desired radionuclide from the rest of the supernatant. This is based on the adsorption and desorption of anions on the resin bed, and was the method used in this study.

The separation of plutonium from the rest of the supernatant matrix was achieved using the following procedure; 1.0 g of sediment from each of the dried samples was weighed into a crucible, then ashed in a furnace at 500 °C overnight to destroy any remaining organic matter (Morris, 1996; Lee and Clark, 2005). The ashed residue was transferred from the crucible to a 100 mL beaker using minimal amounts of 18 MΩ DI. Once cool the ashed residue was leached with 15 mL 3:2 cHCl: $cHNO_3$

by boiling for 3 hours. This acid treatment dissolves any analyte in the solution. The solution was then allowed to cool, with any solids being removed *via* filtration (using Whatman, cellulose, 8µm pore filter paper) into a 100 mL volumetric flask. This was rinsed with 9M HCl until the filtrate ran clear. The filtrate was made up to 100 mL with 9 M HCl to prevent the hydrolysis of Pu^{4+}. The 100 mL stock solution was then decanted into plastic bottles to produce stock solutions ready for spiking and separation. 20 mL of the stock solution was added to a 100 mL beaker and a spike (200 µl ^{242}Pu tracer (0.75 Bq/ml^{-1})) was added to the sample solution prior to evaporating to incipient dryness. Thereafter, the solution was taken up in 20 mL of 9 M HCl and 0.5 mL $cHNO_3$ was added. This addition of $cHNO_3$ ensured any Pu present was in the +4 oxidation state (any Pu^{3+} was oxidised to Pu^{4+} and Pu^{6+} was reduced to Pu^{4+}) as this is the ion which will be held on the resin bed. This ensured that the Pu isotopes present in the sample and the tracer were in the same oxidation state allowing Pu to form the anionic species $[PuCl_6]^{2-}$ which was held on the column (Morris, 1996).

The anion exchange resin was allowed to swell for 30 minutes in 18 MΩ DI, after which it was poured into the column (6 cm x 0.6 cm I.D Bio Rad AG1-X8). To precondition the column, 1 M HCl was then added (5 mL) and run through the column. Thereafter 9M HCl was added (20 mL) and allowed to run through the column preparing it for sample introduction. The sample (20 mL) was then passed through the column. Any Am passed through the resin as the $[AmCl_3]$ species. The resin was then washed with 40 mL 9 M HCl to remove any residual sample solution, this was added in 20 mL quotients and allowed to pass through. 8 M HNO_3 (25 mL) was then added to the column to remove any Fe and U.

Thereafter, 5mL of cHCl was added to remove Th and condition the column for Pu elution. The Pu was eluted with 0.2 M HI/11.1 M HCl (25 mL), reducing Pu^{4+} to Pu^{3+} and desorbing it from the column. 1 mL of 10 % (m/v) $KHSO_4$ carrier solution was added to the Pu fraction. The eluate and the carrier were then evaporated to dryness and 3 mL $cHNO_3$ was added to oxidise any I^- to I_2. The sample was then evaporated to incipient dryness and the $cHNO_3$ treatment repeated. Finally, 3 mL cHCI was added to ensure all the Pu was complexed with Cl^- (to change the column to chloride form). This was evaporated to dryness again to produce a white residue.

2.4.3.2. Electrodeposition of Pu

The cell used for electrolysis of the sample consists of two glass tubes (SV30, Orne Scientific, Manchester) which are connected by a plastic collar. The brass base containing the stainless steel planchette, and a Teflon™ ring were placed into the lower glass tube. Simultaneously, both tubes were twisted into the plastic collar to provide a secure fit which was clamped into place. The cell was then checked for any leaks by adding 18 MΩ DI to the top glass tube. A rubber bung containing the anode was placed on the top ensuring immersion into the solution, and the cell was connected to the power supply. The white Pu fraction obtained from the chemical separation step was then dissolved in electrolyte solution (15 mL 4 % $(NH_4)_2C_2O_4$ in 0.3 M HCI). The sample was then transferred to the electrodeposition cell and the beaker was rinsed with 15 mL 18 MΩ DI and added to the cell. Electrodeposition was carried out at 0.5 A, 20 V for 3 hours. A minute prior to the end, 1 mL NH_3 solution was added to the cell. The power supply was then turned off and the planchette rinsed with a few mL of 18 MΩ DI, C_2H_6O, and C_3H_6O before drying in air. The Pu containing planchette was then sealed in a ziplock PVC bag ready for

analysis on the CANBERRA 7401 α-spectrometer. The samples were counted until a good count rate was observed for each isotope.

Chapter 3
Results and Discussion

3.1. Biogeochemistry of the Ravenglass Sediment Core

The concentrations of major and minor elements (e.g. Al, Si, Mg, K, Ti, Mo, Mn, and Fe) in Ravenglass sediment samples are listed in Appendix 1 and are shown in Figure 9A-H. The concentrations of Mn and Fe (Figure 9G and 9H) have been divided by Al to remove the detrital (non-reactive) fraction (e.g. Shimmield and Pedersen, 1990). The concentrations of 0.5 M HCl extractable Fe (herein reactive Fe) measured in the Ravenglass sediment samples are listed in Appendix 1 and are shown in Figure 9I.

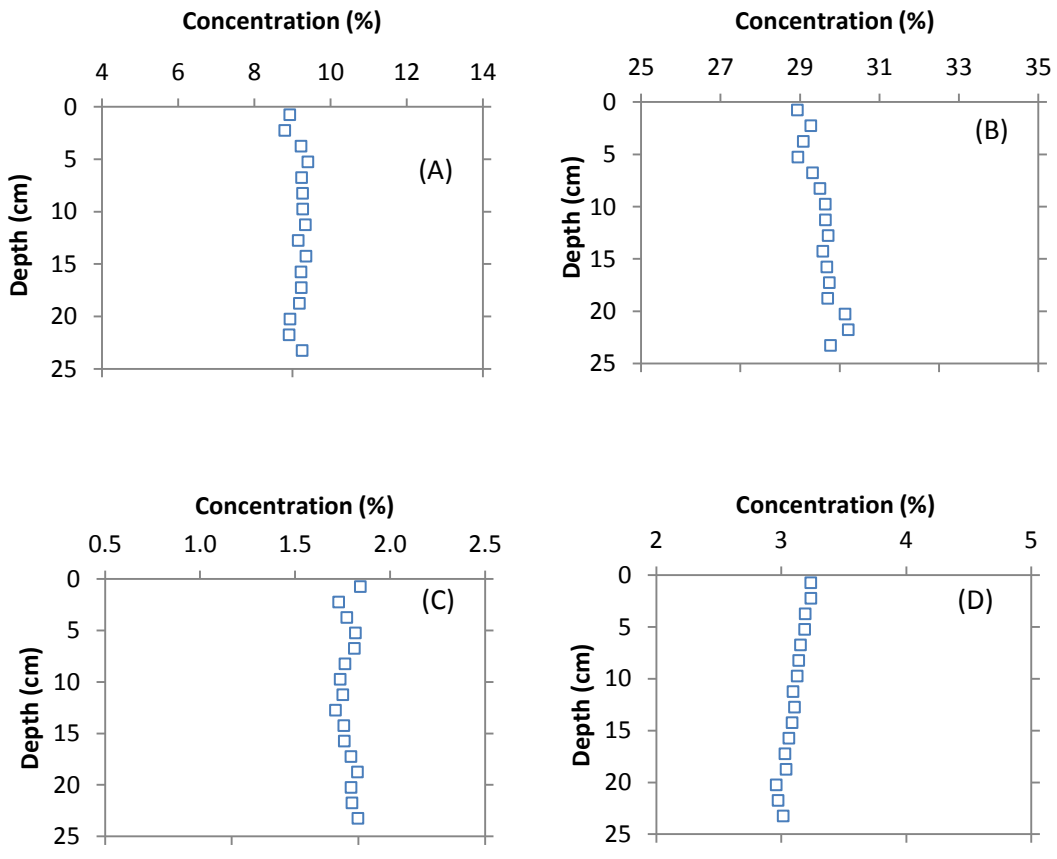

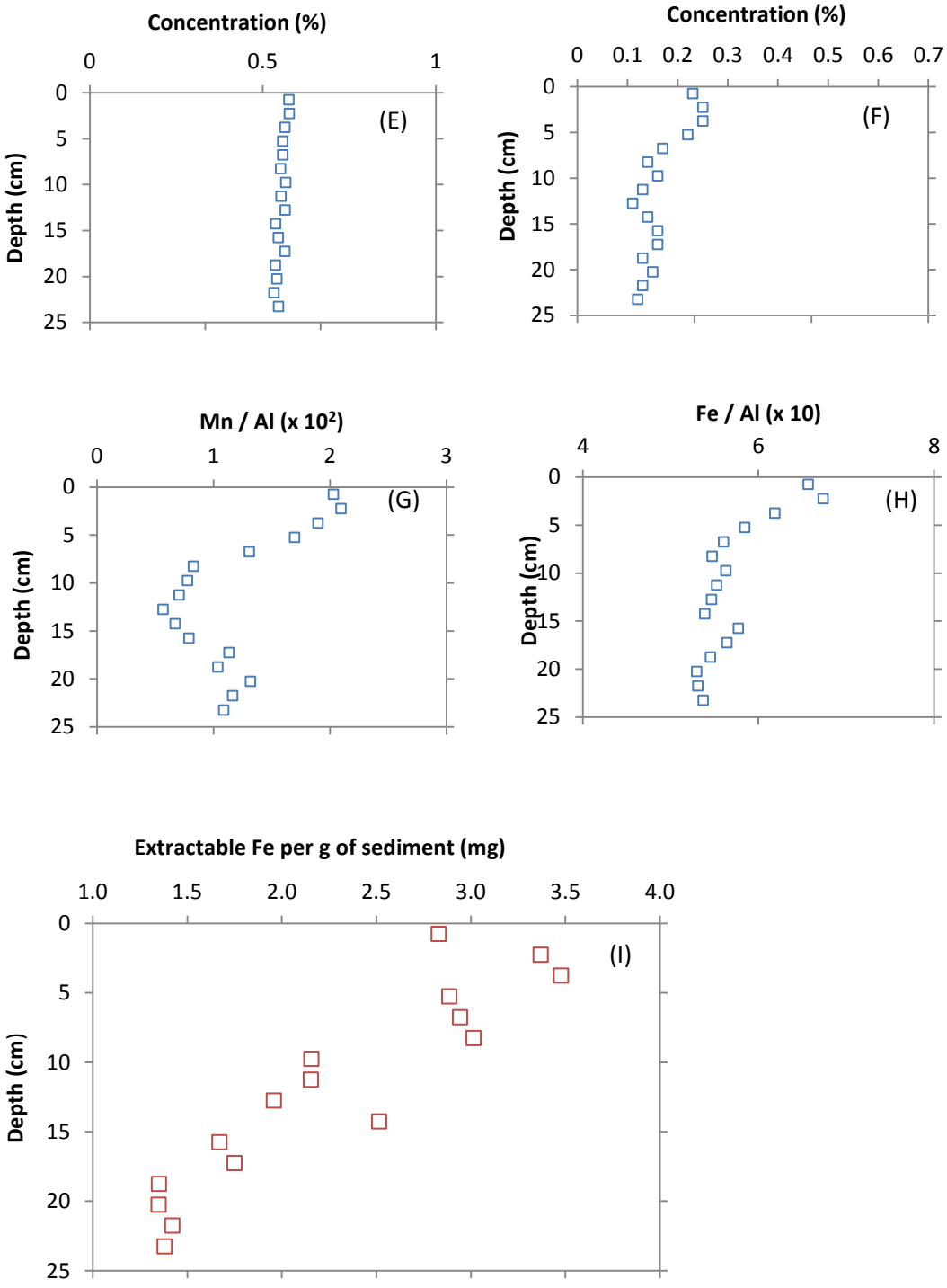

Figure 9. Concentration (wt %) of (A) Al; (B) Si; (C) Mg; (D) K; (E) Ti; (F) Mo ($x10^3$); (G) Mn/Al (x 10^2); (H) Fe/Al (x 10), and (I) extractable Fe (mg g^{-1} of sediment) in Ravenglass saltmarsh sediments from 0-25.5 cm.

As shown in Figure 9A-9F, the distribution of common lithogenic elements (e.g. Al, Si, Mg, K, and Ti) varies little with depth. This suggests that the bulk geology of sedimenting particulates in the Ravenglass estuary are remaining (hitherto) constant with time. In contrast, for Mn and Fe (Figure 9G and 9H), there is clear deviation from this trend. Initially, high Mn/Al ratios (~ 2.0 x 10^3) in the surface sediments decrease until a minimum (~ 0.6 x 10^3) is attained at 12.75 cm (Figure 9G). As the depth increases further, there is then an increase in the Mn/Al ratio until a depth of 18.75 cm is attained. The high concentration of Mn observed in the surface sediments is likely due to the input of freshly precipitated Mn oxy(hydr)oxides. The burial of these phases below the surface oxic zone, and microbially mediated reduction of $Mn^{3+}/Mn^{4+}_{(s)}$ to $Mn^{2+}_{(aq)}$ coupled to the oxidation of organic matter, likely controls the concentration minimum. The deeper increase in the Mn/Al ratio may reflect the precipitation of rhodochrosite or MnS (Shimmield and Pedersen, 1990). For Fe, as the depth of the core increased there was a general decrease in the Fe/Al ratio, ranging from ~ 6.5 x 10 in the surface sediments to ~ 5.2 x 10 below ~ 10 cm. (Figure 9H). Likewise, for extractable Fe, a high concentration (~ 2.5-3.5 mg g^{-1}) was found the surface sediments where oxic conditions dominate. This likely represents a fresh input of ferric oxy(hydr)oxides to the surface sediments. Further, the burial of these phases below the surface oxic zone, and subsequent microbially-mediated reduction of $Fe^{3+}_{(s)}$ to $Fe^{2+}_{(aq)}$ (coupled to the oxidation of organic matter), likely controls the steady decrease in reactive Fe content (down to ~ 1.3 mg g^{-1} below 10 cm) and Fe/Al ratio down-core (Froelich et al., 1979). Tidal pumping of the $Fe^{2+}_{(aq)}$ back into surface sediments followed by oxidation and precipitation of Fe^{3+} phases may also be influencing the observed Fe profiles. Finally, the absence of a subsurface reactive Fe concentration maximum and increase in the

Fe/Al ratio at depth, together with the absence of olfactory evidence for hydrogen sulphide in the field, suggests that sulphate reduction and Fe-sulphide precipitation is insignificant in surface sediments (~ 0-25 cm) of the Ravenglass saltmarsh.

3.2. Contemporary Radionuclide Distribution in the Ravenglass Sediment Cores

The quantity and composition of the authorised discharges to the Irish Sea has varied with time as processes have altered at the Sellafield site. These factors include the type of fuel used in the reactor, its burn-up time, storage time of spent fuel prior to reprocessing, and the method of reprocessing utilised (Mackenzie and Cook, 1997). As a result of these changes each radionuclide has a characteristic, temporal discharge pattern (Figures 10-13B). Early in the site's history (1952-1968) the activity of effluent discharged into the Irish Sea was low. A peak in the effluent activities then occurred in the mid 1970's, and this was followed by a decline in activity towards the end of the discharge history (1978-1992). However the relationship between the radionuclide concentration in the layer of sediment deposited in a particular year and the corresponding quantity of that radionuclide discharged from Sellafield may depend on a number of factors beyond the source term; for example, redistribution within the core due to bioturbation, diffusion or diagenesis; dilution of the contemporary signal by 'older' material corresponding to earlier discharges, changes in particle size distribution, variations in accumulation rate, and variance of sediment transport in the Irish Sea (Kershaw et al., 1990).

The Ravenglass saltmarsh is a site which has been known to accumulate sediments at a slow rate (~ 4 mm yr^{-1}) (Kelly and Emptage, 1992). Therefore a sediment core that

is taken from this area and that is not undergoing bioturbation or post-depositional remobilisation- to a vast extent, will tend to show a resemblance to the activity variation of the authorised discharges (MacKenzie et al., 1994; Kershaw et al., 1990). Any discrepancies which may occur in matching the discharge trend with the radionuclide profile may be due to different 'lag times' experienced by different radionuclides between release from Sellafield and deposition in intertidal sediments or post-depositional modification (Aston and Stanners, 1981; Hamilton and Clarke, 1984).

3.2.1. Caesium

The ^{137}Cs activities measured in the Ravenglass sediments are listed in Appendix 2 and are shown in Figure 10. Down-core, the ^{137}Cs activities ranged from 0.057 kBq kg^{-1} to 5.14 kBq kg^{-1} with the highest activity found in the middle of the core (10.5-12 cm). Initially, close to the surface (0-5 cm), there was a low concentration of ^{137}Cs present (0.35 kBq kg^{-1}). As the depth of the core increased, the concentration of ^{137}Cs steadily increased before reaching the aforementioned maximum. As the depth of the core increased further, the concentration began to decrease until a depth of 18 cm. Thereafter, the concentration of ^{137}Cs slowly decreased reaching a minimum (0.057 kBq kg^{-1}) at 24 cm. As a consequence the sediment core profile shows a well-defined subsurface peak that tails off equally on both sides of the concentration maxima (Figure 10B). On first approximation, the shape of the depth profile is similar in shape to that of the Sellafield discharge record (Figure 10A), resembling the maximum in radionuclide discharge during the mid 1970's. However, the authorised discharge record also shows a minor increase in

activity during 1970-1972 and interestingly, this is not replicated in the sediment core.

The observed deposition of Cs in the Ravenglass sediments and the pseudo-comparability to the effluent discharge record may be due to various physical and biogeochemical processes acting on Cs after it is introduced into the Irish Sea *via* the pipeline. Whilst Cs (a monovalent cation) is a relatively soluble species due to its low charge density (i.e. it does not hydrolyse readily), a small proportion of Cs entering the Irish Sea does tend to associate with marine sediments (Hetherington, 1978). Here, the dominant mechanism removing Cs^{+} from solution is adsorption to particulates and cation exchange reactions at the mineral-surface/solute interface. In particular, clay minerals present in sediments and soils contain weakly bound hydrated interlayer cations (e.g. Ca^{2+}, K^{+}) that can be displayed by cations in solution (i.e Cs^{+}). Consequently, micaceous minerals (e.g. illite) tend to immobolise Cs^{+} or incorporate it into their crystal lattice. As sediments from the Sellafield area have been shown to contain a high content of illite (Kelly and Emptage, 1992), such a reaction could potentially explain the similarity between the Ravenglass sediment Cs profile and the authorised discharge record. With regards to the lack of temporal resolution in the Ravenglass sediment Cs profile; as the transport of Cs from the pipeline to the Ravenglass saltmarsh is time-averaged (Marsden et al., 2006), it is possible that smaller transient patterns in the effluent discharge may not always be seen in the Ravenglass sediment core profile. Indeed, as the majority of the Cs from the pipeline is soluble, ephemeral rapid mass water movement may transport the activity to other areas of the Cumbrian coastline. Smearing of smaller peaks in the Ravenglass core *via* bioturbation may also have acted to mask fidelity between the discharge and sediment record.

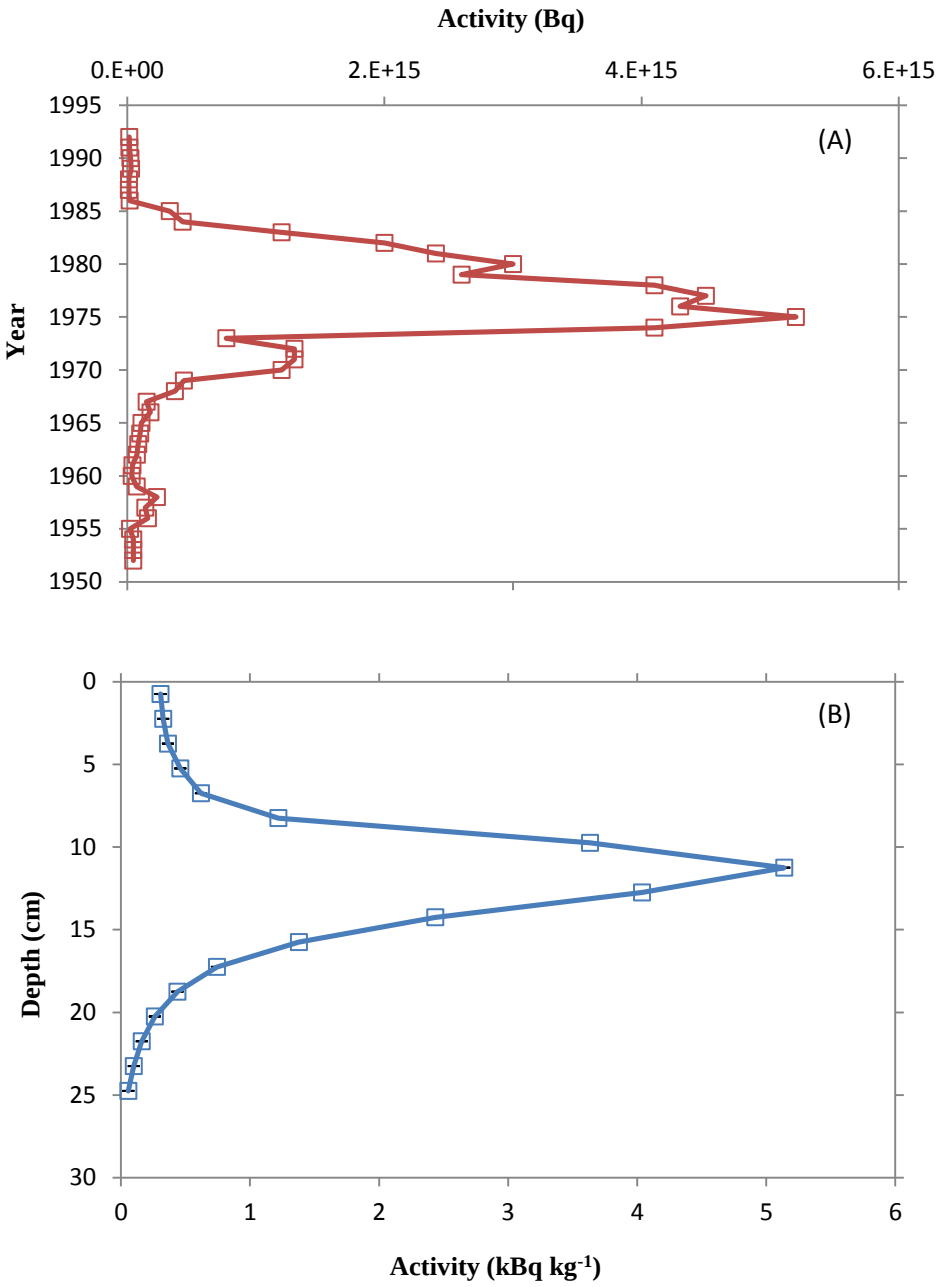

Figure 10. (A) Annual authorised discharge of ^{137}Cs into the Irish Sea from the Sellafield site between 1952-1992 (data from Gray et al., 1995); (B) ^{137}Cs activity profile in the Ravenglass saltmarsh from 0-25.5 cm depth (Appendix 2). Counting errors are ±1σ and if not visible are hidden by the symbol.

3.2.2. Americium

The ^{241}Am activities measured in the Ravenglass sediments are listed in Appendix 2 and are shown in Figure 11. Down-core, the ^{241}Am activities ranged from 0.004 kBq kg^{-1} to 18.3 kBq kg^{-1}. Near the surface of the core (0-5 cm) there was a low concentration of ^{241}Am present (~ 1.14 kBq kg^{-1}). As the depth of the core increased there was a sharp rise in the concentration of ^{241}Am, attaining a maximum at a depth of ~ 12 cm (Figure 11B). As the depth of the core increased further, there was a decrease in the activity of ^{241}Am until a depth of 18 cm. Thereafter, below 18 cm the concentration attained a below detection value until the end of the core. The maximum in activity of the core ^{241}Am profile is sharp and well defined which positively correlates with the maxima of the discharge record (Figure 11). However, as with ^{137}Cs (Figure 10), the authorised ^{241}Am discharge record also shows minor peaks in activity during 1975-1980 that are not replicated in the corresponding sediment core.

The only stable oxidation state of Am in the environment is Am^{3+}. As this species has high charge density it is readily hydrolysed and consequently sorbs to mineral surfaces forming a precipitate [$Am(OH)_3$]. This precipitate is formed by strong inner sphere complexes between the positively charged Am^{3+} ion and negatively charged mineral surfaces (e.g. calcites, layered silicates, α-FeOOH etc.) (Brookshaw et al., 2012). Further, Das and Co-workers (2011) have shown that increasing the pH of aqueous media from 2 to 10 greatly increases the degree of Am^{3+} sorption to mineral surfaces, reflecting an increase in net mineral surface negative charge. As the pH of the Irish Sea is ~ 8.5, suspended particulates and sediments will have a net negative surface charge and this likely encourages Am^{3+} to sorb to mineral surfaces/sediments

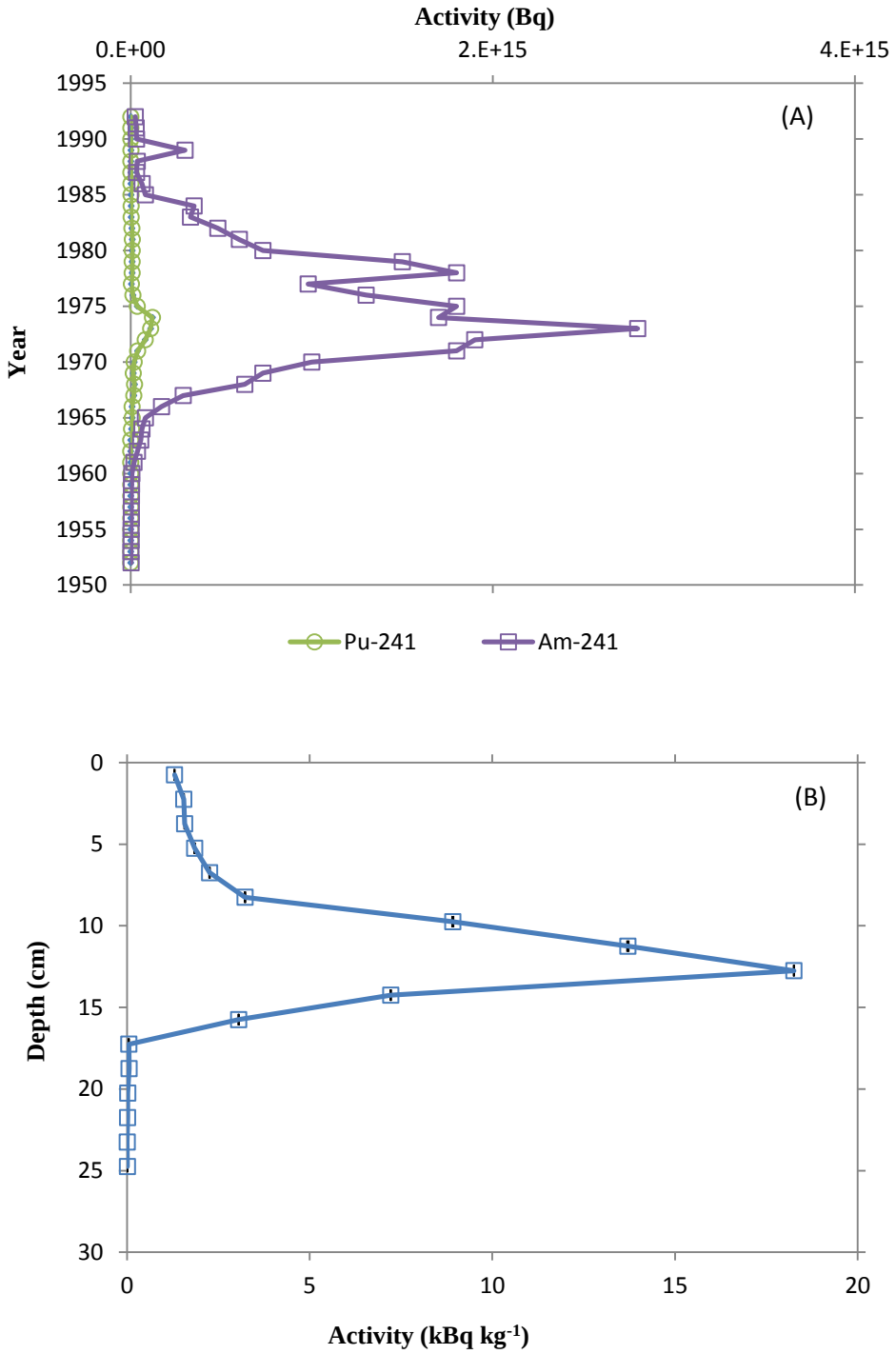

Figure 11. (A) Annual authorised discharge of ^{241}Am and ^{241}Pu activity into the Irish Sea from the Sellafield site between 1952-1992 (data from Gray et al., 1995); (B) Measured activity profile for ^{241}Am in the Ravenglass saltmarsh core (Appendix 2). Counting errors (±1σ) are shown but may be shadowed by markers.

upon release into the Irish Sea. As a consequence, it is perhaps unsurprising that the Ravenglass sediment ^{241}Am profile matches the ^{241}Am discharge history. Strong mineral surface-radionuclide ionic/covalent bonds are also formed at the expense of Am^{3+} losing its surrounding water molecules (Brookshaw et al., 2012) and again this would likely encourage Am to be removed from the effluent to mineral surfaces/sediments in the Irish Sea.

Reflecting the above, Nelson and Lovett (1978) amongst other workers have recognised that lower oxidation state actinides have higher K_d values than higher oxidation state analogues. Indeed, when compared against other actinides, Am has the largest K_d value, (K_d descends in the order: Am/Cm > Pu > Np (Kershaw et al., 1986)). In view of the large K_d value for Am^{3+} it can be suggested that the majority of the Am inventory released to the Irish Sea will have quickly become associated with the offshore sediments. As a result, a simple mechanism of release from pipeline to the incorporation with fine-grained, 'muddy' sediment, to mixing and finally transfer to the estuarine site can be applied to ^{241}Am discharged from Sellafield (Marsden et al., 2006). Further, as suggested for ^{137}Cs, time averaging of ^{241}Am transport to the sampling site, alongside possible bioturbation effects, may have lessened the fidelity of the sediment ^{241}Am profile when compared to the discharge record. Regardless, the absence of significant ^{241}Am below ~ 18 cm in the core suggests that bioturbation/sediment reworking is not excessive at this site, especially at depth.

Finally and importantly, there is likely ingrowth of ^{241}Am to the Ravenglass sediments from the decay of its parent radionuclide, ^{241}Pu, which was present in Sellafield effluents (Gray et al., 1995; Figure 11A). The input of ^{241}Pu to the ^{241}Am signal has not been measured for the Ravenglass sediments used in this study,

however the general trend/shape of the sediment ^{241}Am profile (Figure 11B) would not be expected to change considerably as the discharge history of ^{241}Pu is similar to that of ^{241}Am, with the addition of a high activity spike in the late 1970s.

3.2.3. Plutonium

The measured ^{238}Pu, $^{239/240}$Pu activities in the Ravenglass sediments are listed in Appendix 2 and are shown in Figures 12B and 13B. As both ^{239}Pu and ^{240}Pu emit α-particles at very similar energies (5.105 MeV and 5.123 MeV), the activity of these Pu isotopes are combined to produce a total activity. This is also used to determine the activity ratio between ^{238}Pu and ^{239,240}Pu, which is shown in Appendix 3.

3.2.3.1. Plutonium-239/240

Down-core, the $^{239/240}$Pu activities ranged from 0.027 kBq kg^{-1} to 3.10 kBq kg^{-1} with the highest activity found in the middle of the core at ~ 12.75 cm (Figure 12B). Initially, close to the surface (0-5 cm), there was a low concentration of $^{239/240}$Pu present (~ 0.425 kBq kg^{-1}). As the depth of the core increased, the concentration of $^{239/240}$Pu steadily increased until a depth of ~ 10 cm, after which there was a sharp rise in activity attaining a maximum at a depth of ~ 12 cm. As the depth of the core increased further, there was a sharp decrease in activity from the maximum to a depth of ~ 16 cm. Thereafter, the $^{239/240}$Pu activity steadily decreased reaching a minimum at a depth of ~ 23 cm.

Visually the ^{239,240} Pu profile (Figure 12B) resembles that of the Sellafield discharge record (Figure 12A), with the major features being present. Here, moderately low

levels of activity at enhanced depth in the core are assumed to correspond to early discharges from the site. This is followed by an increase in activity to a well-defined peak, indicative of the change in effluent composition during the mid 1970s, with a final significant decline in ^{239,240}Pu activity being observed in the most recent sections of the sediment core. The distribution of ^{239,240}Pu down the sediment profile is also consistent with other published Pu profiles in the area (e.g. Livens et al., 1994). The authorised discharge profile shows minor peaks in activity during 1975-1980. Again, as with ^{137}Cs and ^{241}Am, these are not replicated in the sediment $^{239/240}$Pu profile.

Of the redox sensitive radionuclides, Pu displays the most complex chemistry in solution, co-existing simultaneously as oxidation states +3 to +6. A range of workers have shown that the principal adsorbed Pu species in the Irish Sea is the reduced form Pu^{4+} with the more mobile, oxidised Pu^{5+} dominating in oxic waters (Pentreath et al., 1984; Kershaw et al., 1984). The lower valence Pu^{5+} species forms a simple cation, M^{5+}, which is readily hydrolysed due to the high charge density of the ion. As a result Pu^{5+} species are lost from solution by reaction with mineral surfaces (Nelson and Lovett, 1978). Conversely Pu^{4+} exists as the dioxo-cation, MO_2^{+}, which is soluble, due to the low charge density of the species couples with its affinity to form carbonato-complexes with common O_2 containing ligands, for example, CO_3^{2-} (Clark et al., 1995). The main mechanism of association between Pu^{4+} and mineral surfaces is *via* sorption, as an inner sphere complex is formed between the mineral phase and Pu^{4+} resulting in a surface precipitate or colloid. Indeed, Pu^{4+} has been recognised to strongly sorb to sediments which are supersaturated in $CaCO_3$, and studies have shown the K_d of Pu^{4+} sorption to calcite is two magnitudes higher than Pu^{5+} (Zavarin et al., 2005). For redox sensitive radionuclides, sorption reactions are also frequently

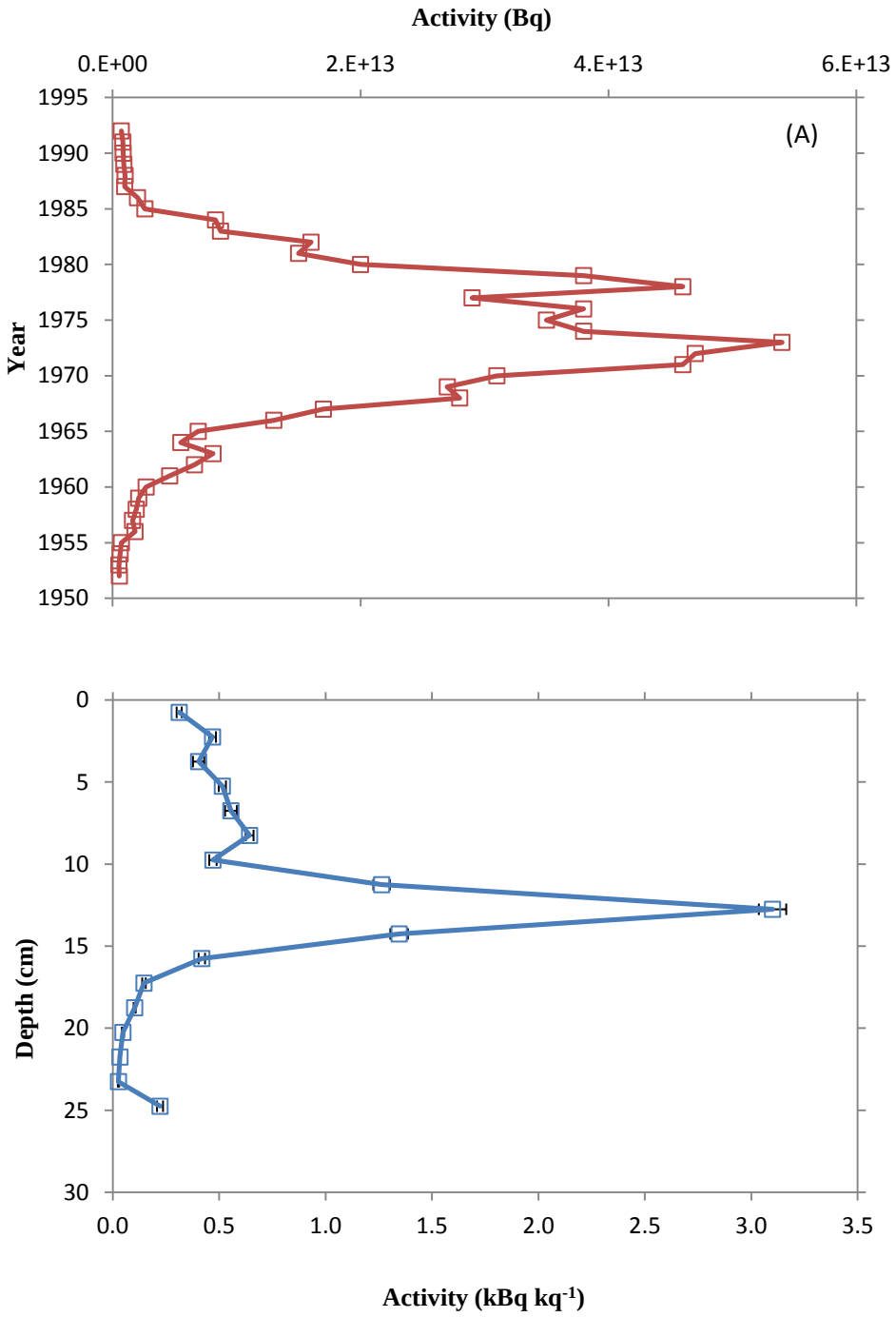

Figure 12. (A) Annual authorised discharge of ^{239,240}Pu into the Irish Sea from the Sellafield site between 1952-1992) (data from Gray et al., 1995); (B) Measured activity profile for ^{239,240}Pu in the Ravenglass saltmarsh core (Appendix 2). Counting errors (±1σ) are shown but may be shadowed by markers.

accompanied by surface mediated redox reactions. The sorption reactions of Pu with manganite (MnOOH) and hausmannite (Mn_3O_4) are facilitated by the surface-mediated reduction of Pu^{6+} to Pu^{5+} and Pu^{3+} (Shaughnessy et al., 2003). As a consequence, on introduction of Pu into the Irish Sea, it is likely that some of it is sorbed (predominantly as Pu^{4+} to regional sediments whilst some is transported from site in regional currents (predominantly as Pu^{5+}).

3.2.3.2. Plutonium-238

The ^{238}Pu activities measured in the Ravenglass sediments are listed in Appendix 2 and are shown in Figure 13. Down-core, the activities of ^{238}Pu ranged from near zero activity to 0.49 kBq kg^{-1} with the highest activity at the centre of the core at ~ 12.75 cm. Initially, close to the surface (0-5 cm), there was a low concentration of ^{238}Pu present (0.08 kBq kg^{-1}). As the depth of the core increased, the concentration of ^{238}Pu also steadily increased until a depth of 11 cm, after which there was a sharp rise in activity attaining the aforementioned concentration maximum. As the depth of the core increased further, there was a sharp fall in the concentration from the maximum to a depth of ~ 14 cm. This was followed by a small decrease in activity to reach the minimum at a depth of ~ 18 cm. Thereafter the near zero activity continued to the bottom of the core. This is broadly comparable to the ^{239,239}Pu profile, however there is no formal authorised discharge history present for ^{238}Pu. Instead workers have calculated a chronology of Sellafield ^{238}Pu discharges by cross referencing several radionuclide concentrations and isotopic ratios, coupled with data on decay-corrected discharges (Kershaw et al., 1990). The differences in geochemical behaviour of different elements can affect their environment dispersal patterns. This can affect the

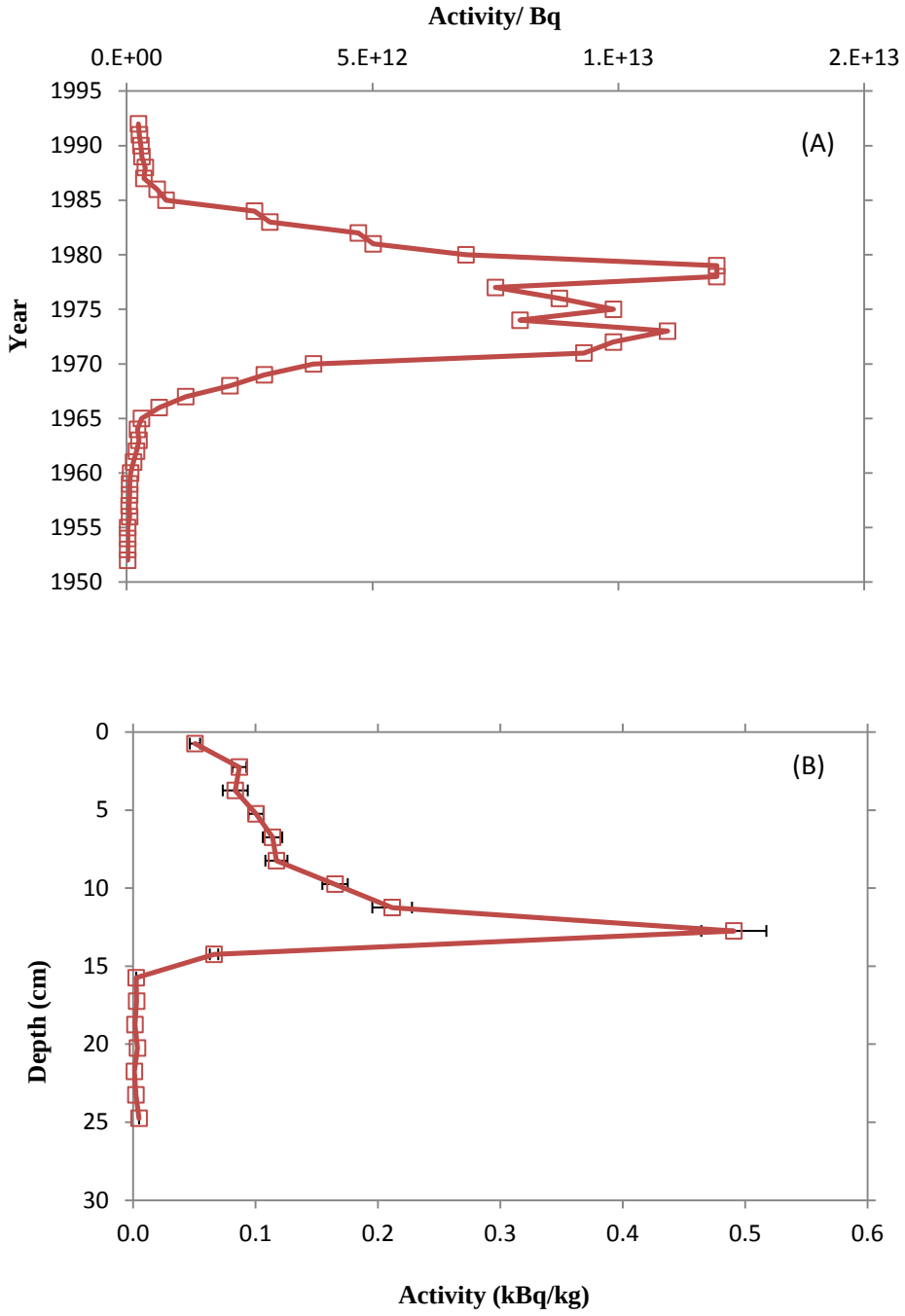

Figure 13. (A) Annual estimate of ^{238}Pu activity into the Irish Sea from the Sellafield site between 1952-1992 (data from Kershaw et al., 1990); (B) Measured activity profile for ^{238}Pu in the Ravenglass saltmarsh core (Appendix 2). Counting errors (±1σ) are shown but may be shadowed by markers.

activity ratios of radionuclides once they have been deposited in the saltmarsh in comparison to the activity ratio in Sellafield effluent. The comparison of isotopic activity ratios eliminates this issue, as isotopic fractionation during environmental processes is negligible (MacKenzie et al., 1994). There is a good agreement between $^{238/239+240}$Pu ratios from the sediment core profile (Appendix 3) and the $^{238/239+240}$Pu ratios from the Sellafield authorised discharge record. If sediment accumulation is occurring at the site then the isotopic ratios for $^{238/239+240}$Pu in the core should be in similar to the isotopic ratio in the discharge history. Indeed, there is a correlation between both sets of isotopic activity ratios. The $^{238/239+240}$Pu for the core ranged from 0.01 to 0.35 with isotopic ratios between 0.03 to 0.35 being observed for the authorised discharge history. This showed that mixing of wastes from different ages is not taking place prior to deposition at the site, provided post-depositional remobilisation is unimportant (MacKenzie et al., 1994). The $^{238/239+240}$Pu activity ratio for the core is comparable to literature; Lee et al, 2005 found ratios of 0.19-0.24 for Irish Sea sediments.

3. 3. Comparison of Contemporary Radionuclide Profiles with Previous Data

The sediment profiles for ^{137}Cs, ^{241}Am, ^{238}Pu, and ^{239,240}Pu in Ravenglass sediments from 1994 (Morris, 1996), 2000 (Marsden et al., 2006), and 2011 (this study) are shown in Figures 14-16. The activities for all the radionuclides from Morris (1996) and Marsden et al., (2000) have been decay corrected accordingly.

3.3.1. Caesium

The maximum concentration of ^{137}Cs in 1994 is illustrated by a sharp peak at a depth of approximately 6.5 cm (23.4 kBq kg^{-1}) (Figure 14). As the depth increased the

activity of ^{137}Cs also decreased, with a minimum being reached at a depth of ~ 16 cm (2.74 kBq kg^{-1}). It can also be seen for Morris's data that the activity of ^{137}Cs does not tail-off to a near zero minimum in comparison to ^{137}Cs activities from 2000 and 2011. This may simply reflect the fact that the analysis of a shallow core by Morris did not permit quantification of the minimum. The core profile for ^{137}Cs determined by Marsden and co-workers for samples collected in 2000 (Figure 14) shows a slower, steadier rise to the maximum (10.7 kBq kg^{-1}), in comparison to Morris. The ^{137}Cs activity maximum at a depth of ~ 16 cm was also much broader in shape, which decreased back to a minimum (0.61 kBq kg^{-1}) at a depth of ~ 29 cm.

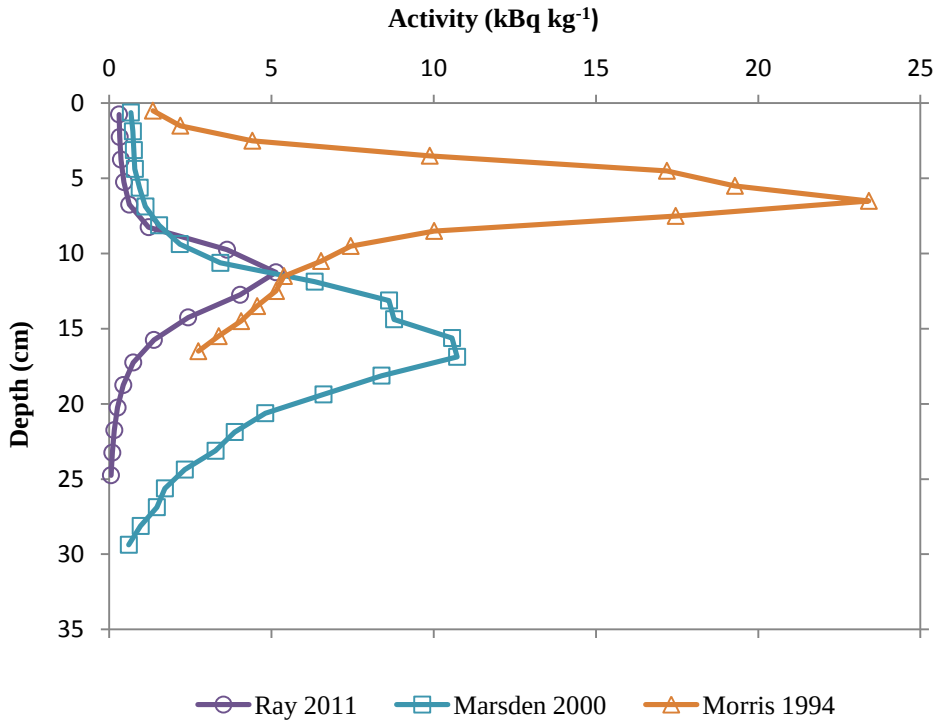

Figure 14. The temporal variation of ^{137}Cs core profiles for Ravenglass estuarine sediments, spanning three decades. Data is taken from this study, Morris (1996), and Marsden et al., (2004).

Comparatively, looking at the three profiles, it seems likely that a simple burial mechanism is taking place at the Ravenglass saltmarsh, without much mixing or post depositional remobilisation of ^{137}Cs taking place. It is clear with all three studies that authorised discharges taken place in the mid 1970's are manifest as pronounced ^{137}Cs signals in Ravenglass intertidal sediments. It may seem that the maximum in activity with time has been buried (from 1994 to 2000), and then has moved upwards to shallower depth (from 2000 to 2011); however this observation likely reflects variation in sedimentation rates across the saltmarsh. As sedimentation is a measure of sediment input and erosion, this can vary across sites significantly, especially in estuaries where there is a non-constant input of marine sediment and erosion rate with the rising and falling tide.

3.3.2 Americium

The maximum concentration of ^{241}Am in 1994 (28.5 kBq kg^{-1}) is shown in Figure 15 as a sharp peak at a depth of ~ 7.5 cm. As the depth increased the activity of ^{241}Am decreased, reaching a minimum at a depth of ~ 16.5 cm (0.24 kBq kg^{-1}). The core profile for ^{241}Am activity determined by Marsden and co-workers for samples collected in 2000 (Figure 15) is similar in shape to that determined by Morris. As the depth of the core was increased there was a steady increase in activity of ^{241}Am, reaching a maximum concentration (27.0 kBq kg^{-1}) at a depth of ~ 18 cm. Thereafter, going deeper down into the core ^{241}Am values decreased attaining a minimum concentration (0.147 kBq kg^{-1}) at ~ 28 cm. The core profile for ^{241}Am activity determined by Marsden and co-workers (Figure 15) showed a slower, steadier rise in activity close to the surface in comparison to Morris. For Marsden, there was also a

slower increase to the maximum ^{241}Am activity followed by a sharp rise, which was illustrated by a small hump at a depth of ~ 16.5 cm.

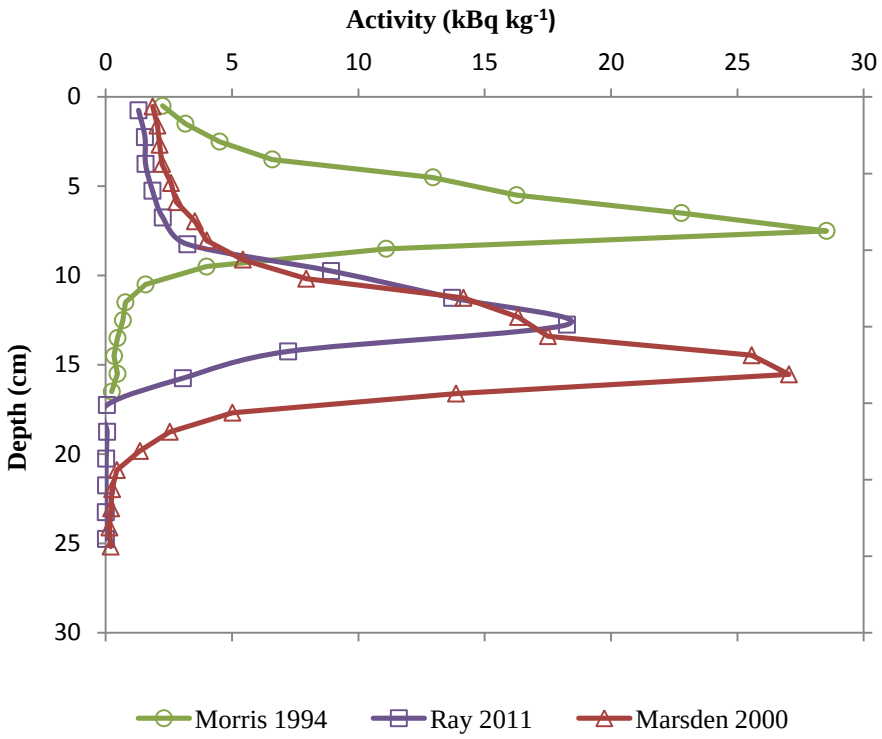

Figure 15. The temporal variation of ^{241}Am core profiles for the Ravenglass sediments, spanning three decades. Data is taken from this study, Morris (1996), and Marsden et al., (2006)

Comparatively, looking at the three profiles, it seems likely that a simple burial mechanism was taking place at the Ravenglass saltmarsh, without much mixing taking place (as discussed for ^{137}Cs). It is clear with all three studies that authorised discharges which took place in the mid 1970's have shown pronounced ^{241}Am signals in Ravenglass intertidal sediments. Further, it may seem that the maximum in activity with time has been buried (from 1994 to 2000), and then has moved upwards to shallower depth (from 2000 to 2011). However, once again this observation likely

reflects variation in sedimentation rates across the saltmarsh. Looking at Figure 14 and 15, it can be seen that there the maximum peaks for ^{137}Cs and ^{241}Am in this study and Morris are constant in separation. This is plausible evidence for burial taking place, as the signals for both radionuclides in this study are being observed at the same distance from the maximum peaks in Morris's study.

3.3.4. Plutonium-239/240

For the oldest core, there was a rapid increase in activity very close to the surface. Within a depth of 5 cm, the ^{239,240}Pu activity reached a maximum (13 kBq kg^{-1}). As the depth was increased further, a second maximum in activity was reached at a depth of ~ 8 cm (15.8 kBq kg $^{-1}$) (Figure 16). Further, going deeper down the core the activity of ^{239,240}Pu decreased to a minimum (0.18 kBq kg^{-1}) at ~ 16 cm. Again, for activities obtained in 2000, there is a slight irregularity in activity with increasing depth. A broad double maxima (15.9 kBq kg^{-1}, 15.2 kBq kg^{-1}) was reached at the centre of the core (~13-18 cm). This maximum was brief as the activity of ^{239,240}Pu decreased rapidly until a depth of 20 cm, before steadily reaching a minimal concentration at ~ 29 cm. Over time the maximum concentration of ^{239,240}Pu has been buried over 6 years due to the readily accumulating nature of the site, this was illustrated by the signal being observed at a lower depth than in 2000, and follows the same trend as the other radionuclides (due to sedimentation). The deviation from the trend at a depth of 7 cm for Marsden's activity data may be due to the mixing of older sediments *via* bioturbation.

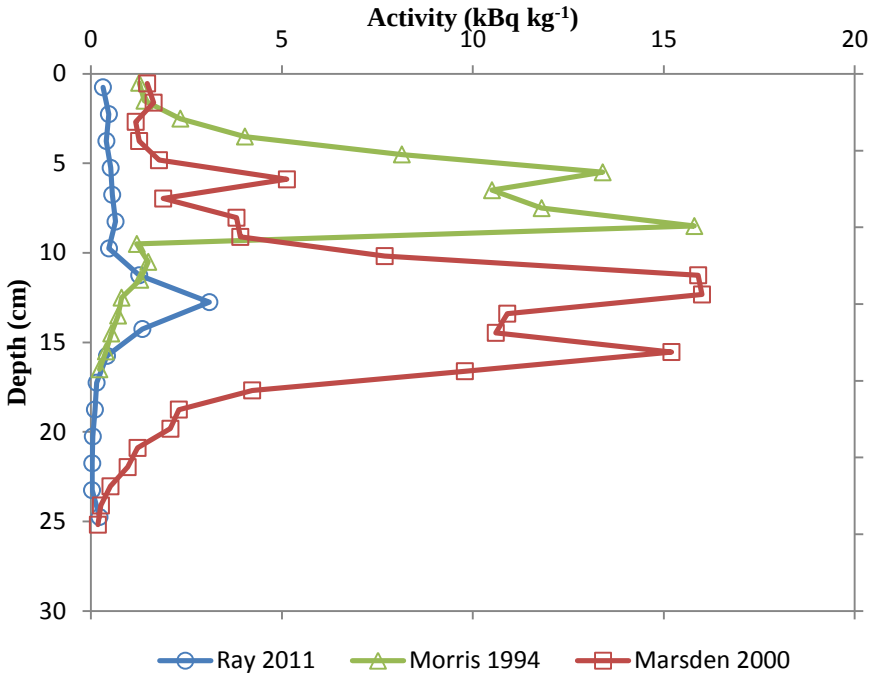

Figure 16. The temporal variation of ^{239,240}Pu core profiles for Ravenglass estuarine sediments, spanning three decades. Data is taken from this study, Morris (1996), and Marsden at al., (2006).

3.3.3. Plutonium-238

The maximum concentration of ^{238}Pu (2.76 kBq kg^{-1}) in 1994 was illustrated by a sharp peak at a depth of 8.5 cm (Figure 17). This high activity decreased with increasing depth, attaining a near zero concentration of ^{238}Pu at a depth of ~ 11 cm. The core profile shown for Marsden for samples collected in 2000 initially displayed an irregular trend at shallow depth (Figure 17), that increased to an activity maximum (3.21 kBq kg^{-1}) at the centre of the core (~13 cm). As the depth of the core was further increased, the activity of ^{238}Pu decreased reaching a concentration minimum at a depth of ~ 28 cm. The smaller maximum peak on the shoulder of the

highest peak may be a result of certain factors; for example, change in particle size, bioturbation, and/or sedimentation.

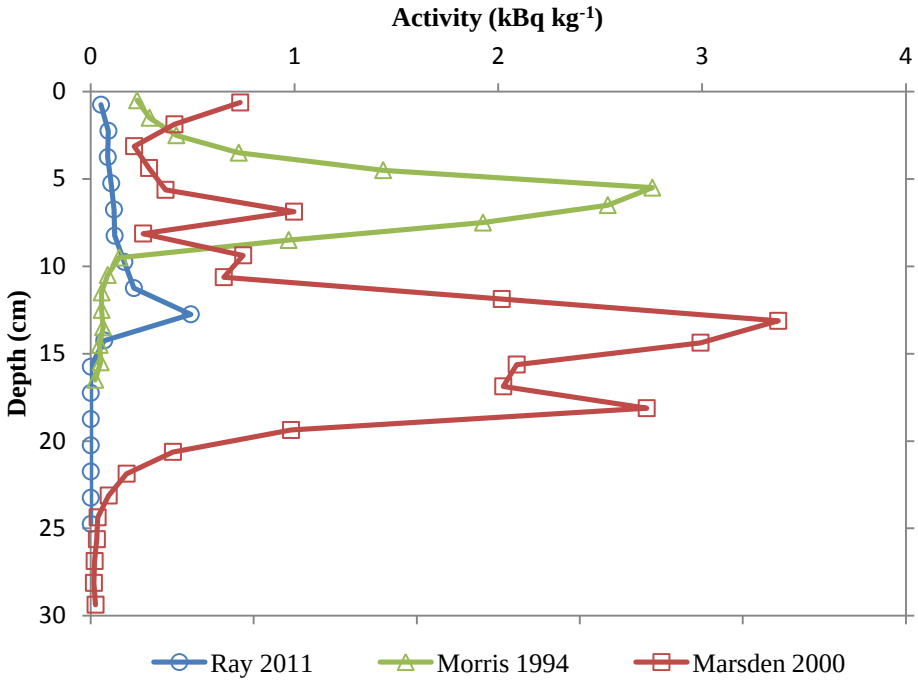

Figure 17. The temporal variation of ^{238}Pu core profiles for Ravenglass sediments, spanning three decades. Data from this study, Morris (1996), and Marsden et al., (2006).

Comparing the three core profiles of ^{238}Pu activity, it is clear with all three studies that authorised discharges which took place in the mid 1970's are manifest as pronounced ^{238}Pu signals in Ravenglass intertidal sediments. As observed previously for ^{137}Cs and ^{241}Am, sedimentation is taking place, which explains the shallower signal for this study. Further, the erratic pattern in the Marsden surface sediments (0-10 cm) may be a result of bioturbation/biogeochemical processes specific to this core.

Ultimately, to understand the mechanism which is taking place at the saltmarsh, a comparison between the activities obtained in 2011 must be made with those of Morris and Marsden. If burial is taking place, then the differences between the maxima in 2011 with that in 1994 and 2000 should, in theory, be the same or very similar. This trend would apply for all the radionuclides. Comparing the maximum activities in 2011 with those of Marsden, 2000, the differences in maximum concentration separation depths for all the radionuclides are, ^{137}Cs (~ 6 cm), ^{241}Am (~ 5 cm), ^{238}Pu (~ 3 cm) and ^{239,240}Pu (~ 1 cm). As these differences vary from 1 cm to 6 cm between radionuclides it is assumed that different sites within the same saltmarsh, with different sedimentation rates were used for this study and the one used in Marsden, 2000. For all the radionuclides the maximum activity signal for 2011 in comparison with 2000 has either remained at the same depth or is observed at shallower depths. The biogeochemistry of the radionuclides suggests they are not mobile, hence they are not moving up the core. Thus it is likely that the site used in Marsden, 2000 is undergoing sedimentation at a slower rate than the site used in 2011. Indeed, Marsden states that the accumulation rate of sediments at the site is 2 mm yr^{-1}, in comparison to the accumulation rate assumed for the site in 2011 (4 mm yr^{-1}). Comparing the maximum activities in 2011 with those of Morris, 1994, the differences for the radionuclides are, ^{137}Cs (~ 5 cm), ^{241}Am (~ 5 cm), ^{238}Pu (~4 cm) and ^{239,240}Pu (~ 4 cm). In contrast to the comparison made previously, the differences in depth separation of maximum activities of the radionuclides between 2011 and 1994 are similar. This indicates that the sample sites used in Morris, 1994 and this study are undergoing sedimentation at a similar rate. Hence the balance between sediment input coming into the sites and the erosion taking place is comparable. This provides good evidence that the activity signals are being buried over time, as new

particulates carrying contaminants from the mud patch are deposited on the saltmarsh.

For each individual core, the maximum activity for each of the radionuclides occurs at a similar depth; 2011 (~12 cm), 1994 (~7 cm), thus showing very little post depositional remobilisation is taking place as all the radionuclides are remaining at a similar depth in the core. For the data obtained in 2000 there is a greater variance in the maximum activities of radionuclides, ranging from 13-18 cm. This may be due to the site specific conditions; particle size, microbiological activity, post-depositional remobilisation of certain elements which are causing the maximum activity of the radioisotopes to be observed at different positions of the depth profile.

Chapter 4
Conclusions and Recommendations for Future Work

4.1. Conclusions

Radionuclides are released from nuclear sites worldwide into aquatic systems. The subsequent redistribution of this radioactivity by physical and biogeochemical processes governs the extent of resulting environmental contamination. This work, and that of previous researchers (Morris, 1996; Marsden et al., 2006), has confirmed that the Cumbrian Ravenglass saltmarsh is a locality that has been contaminated by authorised low-level radioactive waste discharges from the Sellafield site. Further, the sediment core radionuclide profiles determined in this study consistently showed characteristics form the Sellafield discharge record, with the maximum activity of the discharge record in the mid 1970s being replicated in each sediment core profile. This coupled with the similar $^{238}Pu/^{239,240}Pu$ activity ratios for both the sediment core and the discharge record, provides further evidence of the preservation of the discharge history in intertidal sediments. Such observations are also consistent with the conclusions of Morris (1996) and Marsden et al., (2006), suggesting the annual discharge to the Irish Sea was one of the dominant factors dictating the vertical distribution of radionuclides in the core. It must also be recognised that there are many natural processes which have taken place en-route to the saltmarsh, subsequently the time-average of these processes may explain why any transient peaks of the discharge record were not observed in the Ravenglass core analysed in this study.

The importance of biogeochemical processes at the mineral-solute interface are known to influence the speciation, bioavailability and mobility of a contaminant, in particular, for radionuclides such as Pu. Simple mobility retardation mechanisms between a mineral surface and a radionuclide can, in effect, cause the sequestration of a specific particle-reactive radionuclide. Further, post-depositional movement is

dependent on mixing from macrofaunal inhabitants of the saltmarsh, and as there is good comparability of the sediment core with the authorised discharge, this may suggest limited mixing is taking place within Ravenglass sediments. The analysis of the major and minor elements of the Ravenglass sediments show that there is no evidence to suggest that Pu is associated with Fe/Mn phases. If there was an association then the peak concentration of Pu (in the centre of the core) would be expected to be co-located with the Fe/Al and Mn/Al profiles, or a similarity would be expected. The redox inactive Cs ion has been recognised to be incorporated into layered clays in literature (Livens and Loveland, 1988). This is likely controlling Cs behaviour in the Ravenglass sediments discussed in this study and as ^{137}Cs has a reasonably short half-life, in comparison to the actinides, it provides less of a radiological risk in the long-term future.

Finally, the comparison of radionuclide core profiles in this study with previous literature values provides evidence that the Sellafield derived radionuclides are likely being buried in the saltmarsh over time. The different sedimentation rates at the site sampled (in this study and that of Marsden et al., 2006), likely explain nuances in the comparability of data in this specific case. Regardless, the burial of Sellafield radionuclides, if proved correct, is an important finding as it suggests that radiological risk is fixed in place and is becoming less significant with time (i.e. increased burial).

4.2. Limitations and Recommendations for Further Work

A caveat of this work is that another researcher collected the sediment core prior to the author's commencement of study. In retrospect, and after reviewing relevant literature, it became apparent that collection of contemporary materials in the field

under controlled redox conditions would have allowed accurate characterisation of the Ravenglass sediment biogeochemistry. Indeed, with fore thought, the distribution of dissolved O_2, nutrients (e.g. NO_3^-), porewater Mn^{2+}, Fe^{2+}, SO_4^{2-}, and HS^- could have been easily determined. Further, given more time for study, the concentration of other radionuclides in the Ravenglass sediments (e.g. U and Np) could have been determined; thus more fully allowing assessment of radiological risk from contaminated localities surrounding Sellafield. The quantification of ^{234}U and ^{238}U was attempted in this study, however the resulting α-data showed signs of contamination, likely due to the high activities of Pu present in the sample. Neptunium analysis was not attempted due to time constraints.

To build on this work further, cores could be collected from the mud-patch in the Irish Sea and other sites within the Ravenglass Salt Marsh/Esk Estuary. The former would provide contemporary information on the fate of the radionuclides after leaving the pipeline and prior to deposition at the estuary. The analysis of cores from different areas of the Esk estuary would provide knowledge on site-specific biological conditions and their affect on radionuclide distribution. Pore waters could also be collected to note the presence of any soluble/potentially remobilised radionuclides present in the system. Further, other significant radionuclides that were discharged in the Sellafield liquid effluent could be characterised, for example ^{236}U, and the fission product ^{90}Sr. The detection of ^{236}U *via* heavy element Accelerator Mass Spectroscopy (AMS) could be utilised to trace Sellafield derived U. As ^{236}U is exists in nature only in ultra trace quantities and is produced readily in nuclear reactors, the detection of this U isotope acts as a fingerprint for irradiated U (Marsden, 2006). Strontium-90, a high specific activity β- emitter is known to be a highly mobile species in most environments due to its existence as the Sr^{2+} species

(Rod et al., 2010). Reflecting this, it would be beneficial to gain further insight into its behaviour in the West-Cumbrian coastline to better inform assessment of any localised radiological risk. Synchrotron based techniques, for example, the newly commissioned ultra dilute I-20 beamline at the Diamond Lightsource, could also be employed to allow the characterisation of contaminant speciation and local coordination at pseudo-environmental levels. Further, as particulates (e.g. fuel particles) have been recognised in the Sellafield area, their possible identification and characterisation in Ravenglass/mud-patch sediments by micro-focus XAS/XRF techniques could be important to allow accurate assessment of radionuclide sources and mobility. Further, to understand the full affect of potential biogeochemical controls on actinide and fission product behaviour, microcosm experiments with Ravenglass and offshore mud-patch sediments could be utilised to probe radionuclide phase stability (e.g. see Burke et al., 2006 and Law et al., 2010 for examples of potential work).

References

Abdelouas, A. (2006). Uranium Mill Tailings: Geochemistry, Mineralogy, and Environmental Impact. Elements, **2**, 335.

Aller, R.C., and Aller, J.Y. (1992). Meiofauna and solute transport in marine muds. Limnology and Oceanography, **37**, 1018–1033.

Assinder, D.J., Yamamoto, M., Kim, C.K., Seki, R., Komura, K., and Bourne, G.S. (1991). Neptunium in intertidal coastal and estuarine sediments, Journal of Environmenta Radioactivity, **14**, 135-145.

Aston, S.R., and Stanners, D.A. (1982). The transport to and the deposition of americium in intertidal sediments of the Ravenglass estuary and its relationship to plutonium. Environmental Pollution, **3**, 1-9.

Aston, S.R., and Stanners, D.A. (1991). Plutonium transport to and deposition and immobility in Irish Sea sediments. Nature, **289**, 581-582.

Bowen, V. T., Noshkin, V. E., Livingston, H. D., and Volchok, H. L. (1980). Fallout radionuclides in the Pacific Ocean: vertical and horizontal distributions, largely from Geosecs stations. Earth and Planetery Science Letters, **49**, 411-434.

Brookshaw, D.R., Pattrick, A.D., Lloyd, J.R., and Vaughan, D.J. (2012). Microbial effects on mineral-radionuclide interactions and radionuclide solid phase capture processes, Mineralogical Magazine, **76**, 777-806.

Browne, E., Firestone, R.B., and Shirley, V.S. (1986). Table of Radioactive Isotopes, John Wiley and Sons, New York.

Burke, I.T., Boothman, C., Lloyd, J.R., Livens, F.R., Charnock, J.M., McBeth, J.M., and Morris, K. (2006). Reoxidation behaviour of technetium, iron, and sulfur in estuarine sediments. Environmental Science and Technology, **40**, 3529-3535.

Chapman, N.A., and McKinley, I.G. (1987). The geological disposal of nuclear waste. John Wiley and Sons, New York, 10-55.

Charlet, L., Silvester, E., and Liger, E. (2008). N-Compound reduction and actinide immobolisation in surficial fluids by Fe(II): the surface $Fe^{III}OFe^{II}OH$ species, as major reductant. Chemical Geology, **151**, 85-93.

Choppin, G.R., and Wong, P, J. (1998). The chemistry of actinide behaviour in marine systems. Aquatic Geochemisty, 4, 77-101.

Choppin, G.R., Liljenzin, J., and Rydberg, J. (2002). Radiochemistry and nuclear chemistry. Heinemann and Butterworth, Oxford, 516-555.

Choppin, G.R. (2006). Environmental behaviour of actinides, Czech. J. Phys., **56**, 13-21.

Clark, D. L., Hobart, D. E., and Neu, M. P. (1995). Actinide carbonate complexes and their importance in actinide environmental chemistry. Chemical Reviews, **95,** 25–48.

Cleveland, J. M. (1979). Critical review of plutonium equilibria of environmental concern. In chemical modelling in aqueous systems. American Chemical Society. 321-338.

Committee on Radioactive Waste Management (2006) Managing our Radioactive Waste Safely – CoRWM's Recommendations to Government, CoRWM.

Das, D.K., Kumar, S., Pathak, P,N., Tomar, B.S., and Manchanda, V.K. (2011). Sorption of Am(III) on natural sediment: experiment and modelling. Journal of Radioanalytical Nuclear Chemistry, **289**, 137-143.

Day, J.P., and Cross, J.E. (1981). ^{241}Am from the decay of ^{241}Pu in the Irish Sea. Nature, **292,** 33-35.

De Regge, P., and Boden, R. (1984). Review of chemical separation techniques applicable to alpha spectrometric measurements. Nuclear Instruments and Methods in Physics Research, **223**, 181-187.

Dolfing, J., and Tiedje, J.M. (1988). Acetate inhibition of methanogenic, syntrophic benzoate degradation. Applied Environmental Microbiology, **54**, 1871-1873.

Eberth, J., and Simpson, I. (2008). From Ge(Li) detectors to gamma-ray tracking arrays- 50 years of gamma spectroscopy with germanium detectors. Progress in Particle and Nuclear Physics, **60**, 283-337.

Ehmann, W, D., and Vance, D, E. (1991). Radiochemistry and nuclear methods of analysis. John Wiley & Sons, Inc. New York.

Ewing, R.C. (1999). Nuclear waste forms for actinides. Proceedings of the National Academy of Science, **96,** 3432-3439.

Forster, S., Graf, G., Kitlar, J., and Powilleit, M. (1995). Effects of bioturbation in oxic and hypoxic conditions: a microcosm experiment with a North Sea sediment community. Marine Ecology Press Series, **116**, 153–161.

Froelich, P. N., Klinkhammer, G. P., Bender, M. L., Luedtke, N. A., Heath, G. R., Cullen, D., Dauphin, P., Hammond, D., Hartman, B., and Maynard, V. (1979). Early oxidation of organic matter in the pelagic sediments of the eastern equatorial Atlantic Sea. Geochimica Cosmochimica Acta, **7**, 1075-1090.

Garnir, H.P., Weber, G., and Strivay, D. (2008). Resolution and efficiency of silicon drift detectors (SDD) compared with other solid state X-ray systems. X-RAY Spectroscopy.

Gray, J., Jones, S.R., and Smith, A.D. (1995). Discharges to the Environment from the Sellafield site, 1951-1992. Journal of Radiological Protection, **15**, 99-131.

Hahn, O., and Strasseman, F. (1939). Concerning the existence of alkaline earth metals resulting from neutron irradiation. Nature, **27**, 11.

Hamilton, E.I., and Clarke, K.R. (1984). The recent sedimentation history of the Esk Estuary Cumbria: UK: The application of radiochronology. Science of the total Environment, **35**, 325-386.

Hetherington, J.A. (1978). The uptake of plutonium nuclides by marine sediments. Marine Science Communication, **4**, 239-274.

Hodgeson, P.E. (1999). Nuclear Power, Energy and the Environment. Imperial College Press, 51-75.

Hou, X., and Roos, P, (2008). Critical comparison of radiometric and mass spectrometric methods for the determination of radionuclides in environmental, biological and nuclear waste samples. Analytica Chimica Acta, **608**, 105-139.

Hursthouse, A.S., and Livens, F.R. (1993). Evidence for the remobilization of transuranic elements in the terrestrial environment. Environmental Geochemistry and Health, **15**, 163-171.

Ilyin, L.A., Balonov, M.I., and Buldakov, L.A. (1990). Radiocontamination patterns and possible helath consequences of the accident at the Chernobyl nuclear power station. Journal of Radiological Protection, **10**, 13-29.

Joyce, M.J., and Port, S.N. (1999). Environmental Impact of the Nuclear Fuel Cycle. Royal Society of Chemistry, **11**, 73-96.

Kelly, M., and Emptage, M. (1992). Radiological assessment of the Esk estuary. DOE/HMIP/RR/92/015.

Kershaw, P.J., Swift, D.J., Pentreath, R.J., and Lovett, M.B. (1984). The incorporation of plutonium, americium and curium into the Irish Sea seabed by biological activity. Science of the Total Environment, **40**, 61-81.

Kershaw, P.J., Brealey, J.H., Woodhead, D.S., and Lovett, M.B. (1986). Plutonium from European processing operations, its behaviour in the marine environment. Science of the Total Environment, **53,** 77.

Kershaw, P.J., Swift, D.J., and Denoon, D.C. (1988). Evidence of recent sedimentation in the Eastern Irish Sea. Marine Geology, **85**, 1-14.

Kershaw, P.J., Woodhead, D.S., Malcom, S.J, Allington, D.J., and Lovett, M.B, (1990). A sediment history of Sellafield discharges. Journal of Environmental Radioactivity, **12**, 201-241.

Kershaw, P.J., Pentreath, R.J., Woodhead, D.S., and Hunt, G.J. (1992). A review of radioactivity in the Irish Sea, Aquatic Environment Monitoring Report, 5-36.

Kristensen, E., Penha-Lopes, G., Delafosse, M., Valdemarsen, T., Quintana, C.O., and Banta, G.T. (2012). What is bioturbation? The need for a precise definition for fauna in aquatic species. Marine Ecology Progress Series, **446**, 285-302.

Law, G.T., Geissler, A., Lloyd, J., Livens, F.R., Boothman, C., Begg, J., Denecke, M., Burke, I.T., Charnock, J.M., and Morris, K. (2010). Geomicrobiological Redox Cycling of the Transuranic Element Neptunium. Environmental Science and Technology, **44**, 8924-8922.

Lee, M.H., and Clark, S.B. (2005). Activities of Pu and Am isotopes and isotopic ratios in a soil contaminated by weapons-grade plutonium. Environmental Science and Technology, **39**, 5512-5516.

Libes, S.M. (1992). An introduction to marine biogeochemistry. John Wiley & Sons, Inc. Singapore.

Livens, F.R., and Loveland, P.J. (1988). The influence of soil properties on the environmental mobility of caesium in Cumbria. Soil Use and Management, **4**, 69-75.

Livens, F.R., Horrill, A.D., and Singleton, D.L. (1994). Plutonium in estuarine sediments and the associated interstitial water. Estuarine Coastal and Shelf Science, **38**, 479-489.

Livens, F.R., and Sajih, M. (2010). Identification and characterisation of radioactive particles in salt marsh sediments. Materials Science and Engineering, **9,** 1-7.

MacKenzie, A.B., Scott, R.D., and Allan, R.L. (1994). Sediment radionuclide profiles: Implications for mechanisms of Sellafield waste dispersal in the Irish Sea. Journal of Environmental Radioactivity, **12**, 243-265.

MacKenzie, A.B., and Cook, G.T. (1997). Remobilization of Sellafield derived radionuclides and transport from the North-East Irish Sea. Journal of Environmental Radioactivity, **35**, 227-241.

Marsden, O.J., Abrahamsen, L., Bryan, N.D., Day, P., Fifield, K., Gent, C., Goodall, P.S., Morris, K., and Livens, F.R (2006). Transport and accumulation of actinide elements in the near-shore environment: field and modelling studies. Sedimentology, **53**, 237-248.

Morris, K. (1996). Geochemical interactions of transuranic elements in intertidal areas from west Cumbria, UK. Ph.D. Thesis, University of Manchester, Manchester, UK.

Morris, K., Law, G.T., and Bryan, N.D. (2011). Geodisposal of Higher Activity Wastes, Nuclear Power and the Environment. Royal Society of Chemistry, 129-150.

Meitner, L., and Frische, O.R. (1939). Disintegration of uranium by neutrons: a new type of nuclear reaction. Nature., **143**, 239.

Nelson, D. M. and Lovett, M. B. (1978). Oxidation state of plutonium in the Irish Sea. Nature., **276,** 599–601.

Nuclear Decommissioning Authority. (2011). Radioactive Wastes in the U.K: A Summary of the 2010 inventory.

Pantin, H.M. (1991). The sea-bed sediments around the United Kingdom. Research Report of the British Geological Survey.

Pepper, S.E., Bunker, D.J., Bryan, N.D., Livens, F.R., Charnock, J.M., Pattrick, R.A.D., and Collison, D. (2003). Treatment of radioactive wastes: an X-ray

absorption spectroscopy study of the reaction of technetium with green rust. Journal of Colloid and Interface Science, **268**, 408-412.

Pentreath, R.J., Swift, D.J., Kershaw P.J., and Lovett, M.B. (1984). The incorporation of plutonium, americium and curium into the Irish seabed by biological activity. Science of the Total Environment, **40**, 61-81.

Rod, K.A., Um, W., and Flury, M. (2010). Transport of strontium and caesium in simulated Hanford tank waste leachate through quartz sand under saturated and unsaturated flow. Environmental Science and Technology, 44, 8089-8094.

Sajih, M. (2006). Isotopic Composition of Plutonium in Intertidal Sediments, MPhil thesis, University of Manchester, U.K.

Scholkovitz, E.R., and Mann, D.A. (1984). The porewater chemistry of ^{239,240}Pu and ^{137}Cs in sediments of Buzzards Bay, Massachusetts. Geochimica Cosmochimica Acta, **48**, 1107-1114.

Seaborg, G. T., Wahl, A. C., and Kennedy, J.W. (1946). Radioactive element 94 from Deuterons on Uranium. Physical Reviews, 69, 367.

Shaughnessy, D.A., Nitsche, H., Booth, C.H., Shuh, D.K., Waychunas, G.A., Wilson, R.E., Gill, H., Cantrell, K.J., and Serne, R.J. (2003). Molecular interfacial reactions between Pu(VI) and manganese oxide minerals manganite and hausmannite. Environmental Science and Technology, **37**, 3367-3374.

Sharrad, C.A., Harwood, L.M., and Livens, F.R. (2011). Nuclear Fuel Cycles: Interfaces with the Environment- Nuclear Power and the Environment. Royal Society of Chemistry, 40-56.

Shimmield, G.B., and Pedersen, T.F. (1990). The geochemistry of reactive trace metals and halogens in hemipelagic continental margin sediments. Reviews in Aquatic Sciences, **3**, 255-279.

Sholkovitz, E. R. (1983). The Geochemistry of Plutonium in Fresh and Marine water Environments. Earth Science Reviews, **19**, 95-161.

Smith, J.T. (2011). Nuclear Accidents, Nuclear Power and the Environment. Royal Society of Chemistry, 58-78.

Stumm, W., and Morgan, J. J. (1996).Aquatic Chemisty, Chemical Equilibria and Rates in Natural Waters, 3rd Edition , John Wiley & Sons, Inc, New York.

Talvitie, N. A. (1971). Radiochemical determination of plutonium in environmental and biological samples by ion exchange. Analytical Chemistry, **43**, 1827-1830.

Tome, F.V., Rodriguez Blanco, M.P., and Lozano,J.C. (2002). Study of the representativity of uranium and thorium assays in soil and sediment samples by alpha spectrometry. Applied Radiation and Isotopes, **56**, 393-398.

UNSCEAR (2000) United Nation Scientific Committee on the Effects of Atomic Radiation. Sources and Effects of Ionizing Radiation Report, United Nations, New York.

Van Hullebusch, E.D., Lens, P.N.L., and Tabak, H.H. (2005). Developments in bioremediation of soils and sediments polluted with metals and radionuclides, Reviews in Environmental Science and Biotechnology, **4**, 185-212.

Violler, R.., Hunter, P.W., Roychoudhury, K., and Van Cappellen, P. (2000). The Ferrozine method revisted: Fe(II)/Fe(III) determination in natural waters. Applied Geochemistry, **15**, 785-790.

Wilson, P.D. (1996). Nuclear Fuel Cycle: from ore to wastes, OUP, 24-86.

Zavarin, M., Roberts, S.K., Hakem, N., Sawvel, A.M., and Kersting, A.B. (2005). Eu(III), Sm(III), Np(V), Pu(U), and Pu(IV) sorption to calcite. Radiochimica Acta, **93**, 93-102.

Appendices

Appendix 1. The concentration (%) of Al, Si, Mg, K, Ti, Mo (x 10^3), Mn /Al (x 10^2), Fe /Al (x 10), and (I) extractable Fe (mg/g of sediment) in Ravenglass saltmarsh sediments from 0- 25.5 cm

Depth (cm)	Al	Si	Mg	K	Ti	Mo	Mn/Al	Fe/Al	Total Reactive Fe (mg)*
23.25	9.25	29.8	1.83	3.02	0.545	0.120	1.09	5.37	2.83
21.75	8.91	30.2	1.80	2.97	0.532	0.130	1.16	5.31	3.37
20.25	8.93	30.1	1.79	2.96	0.541	0.150	1.32	5.29	3.48
18.75	9.18	29.7	1.83	3.04	0.536	0.130	1.04	5.45	2.89
17.25	9.23	29.7	1.79	3.03	0.564	0.160	1.13	5.64	2.94
15.75	9.22	29.7	1.76	3.06	0.545	0.160	0.789	5.77	3.01
14.25	9.35	29.6	1.76	3.09	0.537	0.140	0.671	5.39	2.16
12.75	9.15	29.7	1.71	3.11	0.565	0.110	0.567	5.46	2.15
11.25	9.34	29.6	1.75	3.09	0.553	0.130	0.705	5.52	1.96
9.75	9.27	29.6	1.74	3.13	0.566	0.160	0.777	5.63	2.51
8.25	9.27	29.5	1.76	3.14	0.551	0.140	0.827	5.47	1.67
6.75	9.24	29.3	1.81	3.15	0.557	0.170	1.31	5.60	1.75
5.25	9.40	28.9	1.82	3.19	0.557	0.220	1.70	5.84	1.35
3.75	9.22	29.1	1.77	3.19	0.564	0.250	1.90	6.18	1.35
2.25	8.80	29.3	1.73	3.24	0.577	0.250	2.10	6.74	1.42
0.75	8.93	28.9	1.84	3.24	0.575	0.230	2.03	6.56	1.38

*mg per g of sediment

Appendix 2**.** The activity of ^{137}Cs, ^{241}Am, ^{238}Pu, $^{239,240}Pu$ in the sediment core (in units of kBq kg^{-1}).

Depth (cm)	^{137}Cs	^{241}Am	^{238}Pu	$^{239,240}Pu$
0 -1.5	0.31 ± 0.002	1.30 ± 0.006	0.05 ± 0.004	0.31 ± 0.01
1.5 -3.0	0.33 ± 0.003	1.55 ± 0.007	0.087 ± 0.006	0.47 ± 0.02
3.0 -4.5	0.36 ± 0.003	1.58 ± 0.007	0.083 ± 0.01	0.40 ± 0.03
4.5 -6.0	0.46 ± 0.003	1.85 ± 0.007	0.1 ± 0.006	0.51 ± 0.02
6.0 -7.5	0.62 ± 0.003	2.26 ± 0.008	0.11 ± 0.008	0.56 ± 0.03
7.5 -9.0	1.22 ± 0.005	3.23 ± 0.009	0.11 ± 0.009	0.64 ± 0.02
9.0 -10.5	3.63 ± 0.008	8.92 ± 0.02	0.16 ± 0.01	0.47 ± 0.02
10.5 -12.0	5.14 ± 0.009	13.7 ± 0.02	0.21 ± 0.016	1.26 ± 0.04
12.0 -13.5	4.04 ± 0.008	18.3 ± 0.004	0.49 ± 0.02	3.10 ± 0.06
13.5 - 15.0	2.44 ± 0.007	7.22 ± 0.009	0.06 ± 0.003	1.35 ± 0.04
15.0 - 16.5	1.38 ± 0.005	3.06 ± 0.004	0.002 ± 0.001	0.42 ± 0.02
16.5 - 18.0	0.74 ± 0.002	0.048 ± 0.003	0.003 ± 0.001	0.15 ± 0.008
18.0 - 19.5	0.44 ± 0.003	0.055 ± 0.003	0.001 ± 0.00	0.10 ± 0.004
19.5 -21.0	0.26 ± 0.002	0.019 ± 0.003	0.003 ± 0.001	0.048 ± 0.005
21.0 - 22.5	0.16 ± 0.002	0.014 ± 0.003	0.001 ± 0.001	0.034 ± 0.002
22.5 - 24.0	0.099 ± 0.002	0.005 ± 0.003	0.002 ± 0.001	0.03 ± 0.003
24.0 -25.5	0.057 ± 0.001	0.01 ± 0.003	0.005 ± 0.001	0.22 ± 0.01

Uncertainties presented are ±1 σ, based on counting errors.

Appendix 3. Activity ratios for $^{238}Pu/\ ^{239,240}Pu$ in the sediment core.

Depth (cm)	$^{238/239,240}Pu$ Activity Ratio
0 -1.5	0.16
1.5 -3.0	0.19
3.0 -4.5	0.21
4.5 -6.0	0.19
6.0 -7.5	0.21
7.5 -9.0	0.18
9.0 -10.5	0.35
10.5 -12.0	0.17
12.0 -13.5	0.16
13.5 - 15.0	0.05
15.0 - 16.5	0.01
16.5 - 18.0	0.02
18.0 - 19.5	0.01
19.5 -21.0	0.07
21.0 - 22.5	0.03
22.5 - 24.0	0.08
24.0 -25.5	0.02